EUROPEAN ORGANIZATION FOR NUCLEAR RESEARCH (CERN)

CERN-EP-2024-234
2024/10/08

CMS-SMP-22-008

Study of same-sign W boson scattering and anomalous couplings in events with one tau lepton from pp collisions at $\sqrt{s} = 13\,\text{TeV}$

The CMS Collaboration*

Abstract

A first measurement is presented of the cross section for the scattering of same-sign W boson pairs via the detection of a τ lepton. The data from proton-proton collisions at the center-of-mass energy of 13 TeV were collected by the CMS detector at the LHC, and correspond to an integrated luminosity of $138\,\text{fb}^{-1}$. Events were selected that contain two jets with large pseudorapidity and large invariant mass, one τ lepton, one light lepton (e or μ), and significant missing transverse momentum. The measured cross section for electroweak same-sign WW scattering is $1.44^{+0.63}_{-0.56}$ times the standard model prediction. In addition, a search is presented for the indirect effects of processes beyond the standard model via the effective field theory framework, in terms of dimension-6 and dimension-8 operators.

Submitted to the Journal of High Energy Physics

*See Appendix A for the list of collaboration members

1 Introduction

The discovery of the Higgs boson [1] provided evidence that fermions and bosons acquire their masses through the Brout–Englert–Higgs mechanism of electroweak (EW) spontaneous symmetry breaking [2–4]. In this framework, vector boson scattering (VBS) processes play a special role. This occurs because in the standard model (SM) the unitarity of the scattering amplitude depends on a cancellation of diagrams involving the mediation of the Higgs boson between longitudinally polarized vector bosons. As a result, the contribution of the longitudinal polarization component to vector boson scattering is very small. Therefore, for even small deviations from the SM couplings of the Higgs boson to the vector bosons, the VBS cross section would diverge from the SM expectations with increasing center-of-mass energy. The measurement of VBS processes thus provides an indirect probe of physics beyond the SM (BSM), even for scenarios in which new resonances are not energetically accessible at the LHC [5]. The theoretical calculation of the effects of different sources of deviations from the SM is sensitive to the method chosen to "unitarize" the process at higher energies [6, 7].

At tree level the VBS cross section is a sum of purely EW terms of order α_{EW}^6, where $\alpha_{\mathrm{EW}} = g_W^2/4\pi$ is the electroweak SU(2) coupling, which leads to a small cross section. Experimental VBS signatures also include irreducible contributions that enter at order $\alpha_{\mathrm{S}}^2\alpha_{\mathrm{EW}}^4$, where α_{S} is the strong coupling. These contributions are referred to as quantum chromodynamics (QCD) irreducible contributions. Typical Feynman diagrams for these processes are shown in Fig. 1.

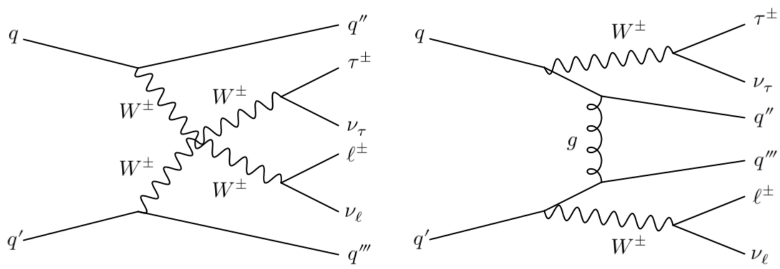

Figure 1: Representative tree-level Feynman diagrams contributing to the process $\mathrm{qq'} \rightarrow \tau^\pm\nu_\tau\ell^\pm\nu_\ell jj$, $\ell = \mathrm{e}, \mu$, leading to cross sections of order α_{EW}^6 (left) and $\alpha_{\mathrm{S}}^2\alpha_{\mathrm{EW}}^4$ (right).

The ATLAS collaboration provided the first evidence of same-sign W pair (SSWW) production via VBS in 2014 by studying final states with electrons and muons [8]. The first observation, in the same final states, was presented by CMS in 2017 [9]. Studies of the VBS production of other combinations of vector bosons have followed [10, 11]. Among the EW-mediated processes, SSWW scattering has the largest cross section and a relatively large cross section ratio between the EW and QCD production modes [12].

The present study of $\mathrm{pp} \rightarrow \mathrm{W^\pm W^\pm} + \mathrm{jets}$ is based on data from proton-proton collisions at $\sqrt{s} = 13\,\mathrm{TeV}$ collected by the CMS experiment at the CERN LHC from 2016 to 2018 and corresponding to an integrated luminosity of $138\,\mathrm{fb}^{-1}$. We investigate a heretofore unexplored final state characterized by the decay of one of the scattered W bosons into a τ lepton that subsequently decays into hadrons (hadronic τ candidate, τ_{h}). The final state thus consists of a charged light lepton $\ell = \mathrm{e}, \mu$, the corresponding neutrino ν_ℓ, one τ_{h} candidate, the corresponding ν_τ, and two jets produced by the quarks recoiling from the production of the W boson pair. Other contributions to this final state could arise from BSM scenarios, especially those that favor the τ over light leptons. Such enhancement may occur through the coupling of the τ lepton to other third-generation particles, or to the Higgs boson because of its larger mass [13–15].

The sensitivity to indirect BSM effects can be probed within the standard model effective field theory framework [16, 17]. This theory is referred to in the literature as "SMEFT", and we adopt the formulation of Ref. [17]. Assuming that new physics with energy scale $\Lambda_{\mathrm{BSM}} \gg \Lambda_{\mathrm{SM}}$ (where Λ_{SM} is a characteristic energy value, such as the Higgs field vacuum expectation value) induces only perturbative effects in VBS processes, the theory is implemented by introducing the following effective Lagrangian:

$$\mathcal{L}_{\mathrm{eff}} = \mathcal{L}_{\mathrm{SM}} + \sum_{D_\alpha > 4} \sum_{\alpha} \frac{c_\alpha^{(D_\alpha)}}{\Lambda_{\mathrm{BSM}}^{D_\alpha - 4}} \mathcal{O}_\alpha^{(D)}, \tag{1}$$

where the operators $\mathcal{O}_\alpha^{(D)}$ are constructed with SM fields at some dimension D_α, and $c_\alpha^{(D_\alpha)}$ are the Wilson coefficients. In this way, the contribution $\mathcal{A}_{\mathrm{BSM}}$ to the total scattering amplitude due to the EFT operators is given by:

$$\begin{aligned} |\mathcal{A}_{\mathrm{BSM}}|^2 = & \sum_{i}^{D_i > 4} \left[\frac{c_i^{(D_i)}}{\Lambda_{\mathrm{BSM}}^{D_i - 4}} 2\,\mathrm{Re}|\mathcal{A}_{\mathrm{SM}}^{*} \mathcal{A}_{\mathcal{O}_i^{(D_i)}}| + \frac{c_i^{(D_i)2}}{\Lambda_{\mathrm{BSM}}^{2(D_i - 4)}} |\mathcal{A}_{\mathcal{O}_i^{(D_i)}}|^2 \right] \\ & + \sum_{j \neq k}^{D_j, D_k > 4} \frac{c_j^{(D_j)} c_k^{(D_k)}}{\Lambda_{\mathrm{BSM}}^{D_j + D_k - 8}} \mathrm{Re}|\mathcal{A}_{\mathcal{O}_j^{(D_j)}}^{*} \mathcal{A}_{\mathcal{O}_k^{(D_k)}}|, < \end{aligned} \tag{2}$$

where the first summation runs over the interference terms between SM and one $\mathcal{O}_i^{(D)}$ operator, the second one over the quadratic contributions of the operators, and the last one over interference between two different operators. The $\mathcal{O}_\alpha^{(D)}$, as well as the corresponding $c_\alpha^{(D_\alpha)}$, are classified according to their dimension D_α to provide a first categorization of their physics effects, as explained below.

Any deviations from SM expectations of the yields observed in the data would provide constraints on the Wilson coefficients, and thus guidance for characterizing BSM effects. Effective field theory interpretations of search outcomes have previously been presented by the ATLAS and CMS Collaborations [12, 18–21]. Assuming that the leptonic universality is not broken by the new operators, the ones with odd dimensions are ruled out. As a consequence, in this study, we investigate operators of dimension 6 (dim-6) and 8 (dim-8), which induce anomalous triple and quartic gauge couplings [22–24]. We refer to any contribution of dimension greater than four as an EFT contribution.

In this paper, we introduce a machine-learning approach to the identification of the single-τ_{h} final state in the SSWW VBS process and perform measurements of the cross section, both for the EW contribution, fixing the QCD contribution, and for the unconstrained EW+QCD combination of these processes. The same approach is implemented to develop models capable of discriminating possible EFT contributions from SM processes.

In the remainder of this paper, Section 2 describes the CMS detector, Section 3 presents the methods for simulating events, and Section 4 describes the particle reconstruction. The selection of signal and control samples is described in Section 5, along with the background estimation, and in Section 6 we discuss systematic uncertainties. The results of the measurement are given in Section 7, and of the EFT interpretation in Section 8. We conclude with a summary in Section 9.

2 The CMS detector

The central feature of the CMS apparatus is a superconducting solenoid of 6 m internal diameter, providing a magnetic field of 3.8 T. Within this magnetic field volume are a silicon pixel and silicon strip tracker, a lead tungstate crystal electromagnetic calorimeter (ECAL), and a brass-and-scintillator hadron calorimeter (HCAL), each composed of a barrel and two endcap sections. Forward calorimeters extend the coverage in pseudorapidity η provided by the barrel and endcap detectors. Muons are detected in gas-ionization chambers embedded in the steel flux-return yoke outside the solenoid. A more detailed description of the CMS detector, together with a definition of the coordinate system used and the relevant kinematic variables, can be found in Ref. [25].

The silicon tracker used in 2016 measured charged particles within the range $|\eta| < 2.5$. For nonisolated particles of transverse momentum p_{T} in the range $1 < p_{\mathrm{T}} < 10\,\mathrm{GeV}$ and $|\eta| < 1.4$, the track resolutions were typically 1.5% in p_{T} and 25–90 (45–150) μm in the transverse (longitudinal) impact parameter. For isolated particles with $p_{\mathrm{T}} = 100\,\mathrm{GeV}$ emitted at $|\eta| < 1.4$, the resolutions are approximately 2.8% in p_{T}, and in impact parameter 10 μm (transverse) and 30 μm (longitudinal) [26]. At the start of 2017, a new pixel detector was installed [27]; the upgraded tracker measured particles up to $|\eta| < 3.0$ with typical resolutions of 1.5% in p_{T} and 20–75 μm in the transverse impact parameter for nonisolated particles of $1 < p_{\mathrm{T}} < 10\,\mathrm{GeV}$ [28].

Events of interest are selected using a two-tiered trigger system [29]. The first level, composed of custom hardware processors, uses information from the calorimeters and muon detectors to select events at a rate of around 100 kHz. The second level, known as the high-level trigger, consists of a farm of processors running a version of the full event reconstruction software, optimized for fast processing that reduces the event rate to around 1 kHz before data storage.

3 Simulated samples

Monte Carlo (MC) simulation is used in the analysis for the design of the event selection, evaluation of signal efficiencies, and estimation of some backgrounds. The EW VBS signal samples are simulated at leading order (LO) with six EW and zero QCD vertices with the MADGRAPH5_aMC@NLO v2.6.5 generator [30], requiring a final state with $\ell\nu_{\ell}, \tau\nu_{\tau}$ pairs from the decays of the two W bosons (Fig. 1, left). The MADGRAPH5_aMC@NLO generator is also used to simulate the QCD-mediated SSWW process, which is generated at LO with up to three additional partons in the matrix element calculations that have at least one QCD vertex at the tree level (Fig. 1, right). In the phase space of interest, the LO cross section, measured with MADGRAPH5_aMC@NLO for the EW VBS processes is 0.0287 pb, and for the residual QCD-mediated contribution is 0.0223 pb. The interference between the SSWW EW and QCD diagrams, including the terms of order $\alpha_{\mathrm{S}}\alpha_{\mathrm{EW}}^{5}$, contributes less than 4% to the inclusive cross section for the EW signal over the phase space region of interest of the analysis [31], and is therefore neglected.

A complete set of next-to-LO (NLO) QCD and EW corrections for the SSWW scattering processes, described above in the leptonic decay channel for each W boson, have been computed as a function of the invariant mass of the VBS jet system [31–33]. They reduce the LO cross section of the EW SSWW process by 10–15%, with the correction increasing in magnitude with increasing dilepton and dijet invariant masses.

The effects of the EFT dim-6 and dim-8 operators are simulated with MADGRAPH5_aMC@NLO at LO. For the dim-6 class, we introduce five bosonic operators acting on the scattering of the W bosons ($\mathcal{Q}_{W}$, $\mathcal{Q}_{HW}$, $\mathcal{Q}_{HWB}$, $\mathcal{Q}_{H\Box}$, $\mathcal{Q}_{HD}$, where the second subscript in $\mathcal{Q}_{H\Box}$ refers to the d'Alembertian that appears in the operator), two fermionic operators acting on contact interactions between fermions ($\mathcal{Q}_{ll}^{(1)}$, $\mathcal{Q}_{qq}^{(1)}$), and four mixed operators acting on interactions between massive bosons and fermions ($\mathcal{Q}_{Hl}^{(1)}, \mathcal{Q}_{Hq}^{(1)}$, $\mathcal{Q}_{Hl}^{(3)}$, $\mathcal{Q}_{Hq}^{(3)}$), defined in the Warsaw basis [17] via the

SMEFTSIM [34, 35] package. For the dim-8 category, we introduce nine operators modifying the interaction between two scattering W bosons ($\mathcal{O}_{S0}$, $\mathcal{O}_{S1}$, $\mathcal{O}_{S2}$, $\mathcal{O}_{M0}$, $\mathcal{O}_{M1}$, $\mathcal{O}_{M7}$, $\mathcal{O}_{T0}$, $\mathcal{O}_{T1}$, $\mathcal{O}_{T2}$) defined in the Eboli basis [36]. In both cases, the effects of the new EFT operators are evaluated and stored using the MADGRAPH5_aMC@NLO reweighting technique [37], and no LO-to-NLO correction is imposed on their contribution.

The POWHEG v2 generator [38–40] is used to simulate, at NLO accuracy in QCD, the following processes: production of $\mathrm{t\bar{t}}$ pairs in which each t quark decays to a b quark and a lepton pair (dileptonic $\mathrm{t\bar{t}}$); tW; Higgs boson production mediated by gluon-gluon fusion; and diboson production. Production of $\mathrm{t\bar{t}W}$, $\mathrm{t\bar{t}Z}$, $\mathrm{t\bar{t}}\gamma$, triple vector boson, vector boson associated with a Higgs boson, and Drell–Yan background events are simulated at NLO accuracy in QCD using the MADGRAPH5_aMC@NLO generator. The tZq process is simulated at NLO in the four-flavor scheme using MADGRAPH5_aMC@NLO. We generally refer to ZZ, Zγ, Wγ, WZ, tribosons, associated production of a quark-antiquark top pair with a γ, Z, or W boson, and tZq processes as "others". The remaining backgrounds, excluding DY, are collectively referred to as "opposite sign" (OS), since they enter the final event selection when the charge of one of the leptons in the final state is misreconstructed.

The NNPDF3.1 next-to-NLO [41] parton distribution functions (PDFs) are used in the simulation of the background and signal samples. The generators used for signal and background processes are interfaced with the PYTHIA 8.306 [42] program, with the CP5 tune [43], to model parton showering and hadronization.

Additional collisions in the same or adjacent bunch crossings (pileup) are included by superimposing simulated minimum bias interactions onto the hard-scattering process, with a multiplicity distribution matching the one that is observed in the data. Simulated events are propagated through the full GEANT4-based simulation [44] of the CMS detector.

4 Event reconstruction

Events are selected for the signal measurement and the estimation of most of the backgrounds that have passed a trigger requiring the presence of either: one muon with $p_{\mathrm{T}} > 24\,\mathrm{GeV}$ in 2016 and 2018 and $p_{\mathrm{T}} > 27\,\mathrm{GeV}$ in 2017; or one electron with $p_{\mathrm{T}} > 27\,\mathrm{GeV}$ in 2016 and $p_{\mathrm{T}} > 32\,\mathrm{GeV}$ in 2017 and 2018. Data are selected for the additional control samples used for background estimation that were recorded with triggers requiring the presence of either a jet with $p_{\mathrm{T}} > 40\,\mathrm{GeV}$ or a jet p_{T} sum $H_{\mathrm{T}} > 350\,\mathrm{GeV}$.

Particle candidates are processed with an optimized combination of all subdetector information using the CMS particle-flow (PF) algorithm [45] that reconstructs and identifies each individual particle in the event. The missing transverse momentum vector $\vec{p}_{\mathrm{T}}^{\mathrm{miss}}$ is defined as the projection onto the plane perpendicular to the beam axis of the negative vector sum of the momenta of all reconstructed PF objects in an event. Its magnitude is referred to as $p_{\mathrm{T}}^{\mathrm{miss}}$.

Jets are reconstructed by clustering PF candidates using the anti-k_{T} jet finding algorithm [46, 47] with a distance parameter of 0.4. Jets are calibrated in the simulation, and separately in data, accounting for energy deposits of neutral particles from pileup and any nonlinear detector response. The effect of pileup is mitigated through a charged-hadron subtraction technique [48] that removes the energy of charged hadrons not originating from the primary vertex (PV) of the event. Corrections to jet energies to account for the detector response are propagated to $p_{\mathrm{T}}^{\mathrm{miss}}$. Jets are required to have $p_{\mathrm{T}} > 30\,\mathrm{GeV}$, $|\eta| < 5$, and to meet jet quality criteria with measured efficiencies that are almost 100%, for both data and simulated samples [49, 50].

The PV is taken to be the reconstructed vertex with the largest value of summed physics-object p_{T}^2, as described in Section 9.4.1 of Ref. [51].

A deep neural network-based tagger, DEEPJET [52–54], is used to identify jets stemming from the hadronization of b quarks, utilizing information from the tracks, neutral particles, and the secondary vertices within the jet. The efficiency and purity of the resulting "b jets" are classified in terms of various working points. The analysis uses a medium working point that correctly identifies b jets with an efficiency of about 70%, and a loose working point with an efficiency of about 85%. The misidentification rates for gluon or light-flavor quark jets for these two working points are 1.0% and 10%, respectivsely.

Electrons (muons) are reconstructed by associating a track reconstructed in the tracking detectors with a cluster of energy in the ECAL (track in the muon system). The candidates are required to originate from the PV, pass quality selection criteria, and be isolated from other activity in the event. For this purpose we define a lepton relative isolation variable I_{rel} based on the energy deposited on a cone $\Delta R = \sqrt{(\Delta\eta)^2 + (\Delta\phi)^2} = 0.3\ (0.4)$ around the electron (muon). Specifically, $I_{\mathrm{rel}} = (E_{\mathrm{ch}} + E_{\mathrm{nh}} + E_{\mathrm{ph}} - 0.5\, E_{\mathrm{ch}}^{\mathrm{PU}}) / p_{\mathrm{T}}$, where E_{ch} is the transverse energy deposited by charged hadrons from the PV, E_{nh} and E_{ph} are the transverse energies of the neutral hadrons and photons, respectively, and p_{T} is the electron or muon transverse momentum. The term $0.5\, E_{\mathrm{ch}}^{\mathrm{PU}}$ accounts for the contribution of neutral particles from pileup vertices, taken as half the energy of the charged particles from pileup vertices.

The quality criteria for the light lepton selection are based on the isolation from other particles in the event and the impact parameter of the candidate with respect to the PV, implemented via multivariate discriminators. In this analysis we make use of both "loose" and "tight" working points of these discriminators. The efficiency for loose (tight) electrons is 90 (80)% [55]. The corresponding efficiencies for muons are 99 (95)% [56].

For a loose electron (muon) we require $p_{\mathrm{T}} > 15\,\mathrm{GeV}$ and $|\eta| < 2.5\,(2.4)$ and $I_{\mathrm{rel}}^{\mathrm{electron}} < 0.20$ ($I_{\mathrm{rel}}^{\mathrm{muon}} < 0.40$). For a tight electron (muon), the criteria are $p_{\mathrm{T}} > 30\,\mathrm{GeV}$ (35 GeV for electrons in 2017 and 2018), and $I_{\mathrm{rel}}^{\mathrm{electron}} < 0.08$ ($I_{\mathrm{rel}}^{\mathrm{muon}} < 0.15$).

Hadronically decaying τ leptons τ_{h} are reconstructed from jets using the hadrons-plus-strips algorithm [57], which combines 1 or 3 tracks with energy deposits in the calorimeters to identify the τ decay modes. Neutral pions are reconstructed as strips with dynamic size in the (η, ϕ) plane from reconstructed electrons and photons, where the strip size varies as a function of the p_{T} of the electron or photon candidate. To furhter distinguish genuine τ_{h} decays from jets originating from the hadronization of quarks or gluons, and from electrons or muons, we make use of the DEEPTAU algorithm [58]. Information from all individual reconstructed particles near the τ_{h} axis is combined with properties of the τ_{h} candidate and the event to provide separate discriminators against hadronic jets (D_j), electrons (D_e), and muons (D_μ). Similarly to the selection of electrons and muons, we employ a loose set of criteria to select τ_{h} with $p_{\mathrm{T}} > 30\,\mathrm{GeV}$, $|\eta| < 2.3$, and satisfying D_j, D_e, D_μ working points for which the genuine τ_{h} identification efficiencies are 70, 98, and 99.5%, respectively. We also make use of a working point with a tighter D_j threshold, for which the identification efficiency for genuine τ_{h} is 50%.

5 Analysis strategy and background estimation

The analysis targets the VBS production of SSWW, with one of the W bosons decaying to a τ lepton and the other into a μ or an e, in association with two jets originating from the scattered incoming partons. Events are first selected by requiring one electron or muon, one τ_{h} candidate, in each case satisfying the tight identification criteria, no additional loose leptons (e, μ, or τ_h candidates), and at least two jets with a pseudorapidity separation $|\Delta\eta| > 2.5$. Among all the possible jet pairs that satisfy the latter requirement, the pair with the highest invariant mass m_{jj} is chosen. We further define the signal region (SR) and several control regions (CRs) to estimate and validate the background predictions, as specified in the following paragraphs. All of these regions are disjoint, and for each of them we require the presence of exactly one tight light lepton and one tight τ_h, rejecting events with additional light leptons or τ_h classified as loose.

The SR is designed to enhance the yield of the VBS signal while minimizing that of the background. Events with a same-sign $\ell\tau_h$ pair, $p_T^{miss} > 50\,GeV$, and $m_{jj} > 500\,GeV$ are selected. In this region, almost 95% of the background events are contain nonprompt lepton candidates, which arise from jets misreconstructed as e, μ, or τ_h, including genuine leptons from the decays of hadrons within jets. About 2% of background events arise from $Z/\gamma^* +$ jets and 1% from dileptonic $t\bar{t}$ production.

Nonprompt leptons are produced mainly by QCD-mediated multijet, associated W + jets, and hadronic and semileptonic $t\bar{t}$ production. They are estimated from data CRs by the "pass-fail" method described in detail in Ref. [59]. This method estimates the probability that a nonprompt lepton passes the tight selection criteria by using a region depleted of prompt leptons to determine transfer factors, functions of their p_T and η. These are then used to calculate the nonprompt contributions in the main SRs and CRs, applying them to auxiliary regions defined as the SRs and main CRs, but requiring that at least one of the light lepton and τ_h pass the loose selection, while failing the tight one.

For this background source, we define two CRs: the "QCD-enriched" CR and the "nonprompt" CR. To define these CRs, the transverse mass $m_T(\ell, p_T^{miss})$ of the system comprising the light lepton and p_T^{miss} is introduced as follows:

$$m_T(\ell, p_T^{miss}) = \sqrt{2 p_T^{\ell} p_T^{miss} [1 - \cos \Delta\phi]}, \tag{3}$$

where $\Delta\phi$ is the azimuthal separation between the lepton momentum vector and $\vec{p}_T^{miss}$. The QCD-enriched CR is used to perform the first step of the nonprompt-lepton background estimations; it contains events with only one loosely identified lepton (e, μ, τ_h), $p_T^{miss} < 50\,GeV$, and $m_T(\ell, p_T^{miss}) < 50\,GeV$ selected from data collected with a jet-based trigger. The nonprompt CR serves to validate the yield estimate from the pass-fail method; it contains events with an SS $\ell\tau_h$ pair and $p_T^{miss} < 50\,GeV$. Lepton candidates in this CR arise mainly from W + jets and QCD multijet production. The data and estimated background m_{jj} distributions are compared in the nonprompt CRs for the electron and muon final states in Fig. 2. The background yields are evaluated before ("pre-fit") the maximum likelihood (ML) fit introduced at the end of this section. The plots show that the data generally agree with the prediction within uncertainties.

Finally, we define $t\bar{t}$ and OS CRs to constrain the MC simulations of these background sources. Events with an OS $\ell\tau_h$ pair and no loose b-tagged jets are selected for the OS CR; events with an OS $\ell\tau_h$ pair, at least one "medium" b-tagged jet, and $p_T^{miss} > 50\,GeV$ are selected for the $t\bar{t}$ CR. Both the $t\bar{t}$ and OS CR are included in the simultaneous ML fit along with the SR. A summary of the analysis phase space with the definitions of the SR and CRs is given in Table 1, with the exclusion of the QCD-enriched CR.

Because of the large background and complex signal topology, sets of significant features to separate signals and backgrounds are combined in three machine-learning discriminators, each targeting a different signal. The discriminators are the outputs of feed-forward deep neural

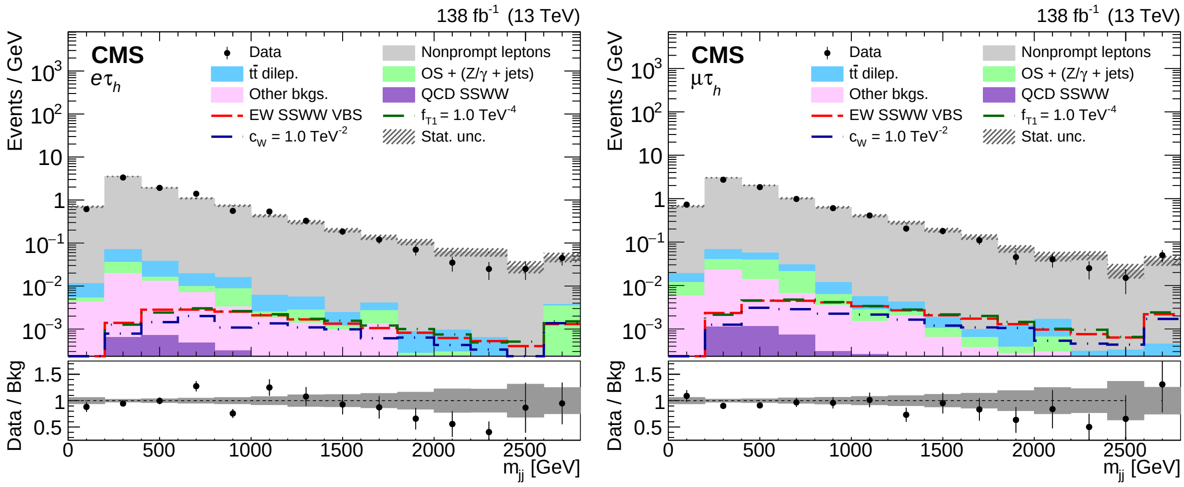

Figure 2: Distributions in the invariant mass of the dijet system for the data and the pre-fit background prediction for the (left) $e\tau_h$ and (right) $\mu\tau_h$ nonprompt CRs. The stacked filled histograms show the background components and the overflow count is included in the last bin. The expectations for the EW SSWW signal, the $\mathcal{O}_W$ dim-6 operator with $c_W = 1\,\text{TeV}^{-2}$, and the $\mathcal{Q}_{T1}$ dim-8 operator with $f_{T1} = 1\,\text{TeV}^{-4}$ are shown by the red, blue, and green lines, respectively. For the latter two, the interference with SM and pure EFT contributions are summed together with the SM contribution. The hatched error band shows the bin-by-bin statistical uncertainty. The lower panels show the ratio of data to the total background prediction, with statistical uncertainties indicated by error bars and hatched shading, respectively. In all the panels, the vertical bars represent the statistical uncertainty assigned to the observed number of events.

Table 1: Definitions of the SR and the four CRs. The ✓ symbol indicates that the requirement described in the column heading is applied in that region, whereas the × symbol means that the opposite selection is applied. T refers to the tight selection rule, L refers to the loose selection rule. The SR and three CRs (nonprompt, $t\bar{t}$, OS) are selected from an inclusive lepton trigger.

Region	1 T ℓ, 1 T τ_h, any L ℓ/τ_h	>= 2 jets with $\lvert\Delta\eta\rvert > 2.5$	SS ℓ, τ_h	p_T^{miss} >50 GeV	Additional requirements
SR	✓	✓	✓	✓	m_{jj} >500 GeV
Nonprompt CR	✓	✓	✓	×	
$t\bar{t}$ CR	✓	✓	×	✓	b-tagged jet (“medium”)
OS CR	✓	✓	×	✓	b-tagged jet veto (“loose”)

networks (DNNs). The three DNN models are devised to separate the SM VBS (SM DNN), EFT dim-6 (dim-6 DNN), and EFT dim-8 (dim-8 DNN) from the SM background processes. In particular, for the first EFT DNN model the signal is represented by a balanced mixture of EFT linear and quadratic contributions weighted with unity values for c_{HW} and c_W. For the second model a balanced mixture of linear and quadratic contributions from all the dim-8 EFT operators included in the study is considered, with the corresponding Wilson coefficient values approximately equal to the 95% confidence level (CL) limits obtained performing a statistical fit with the variable $m_{\circ 1}$ defined in Eq. (5) below. In both cases, the SM SSWW VBS contribution is considered part of the background sample. The optimized models consist of 1, 2 and 4 hidden layers. Adam Optimizer [60], early stopping, dropout, and L2 regularization [61] techniques are utilized to avoid the overfitting effect, consisting of excessive adaptation to training data of the DNN model.

The sets of input variables for the DNNs, detailed in Table 2, are each constructed with a dedicated optimization that includes some quantities introduced to exploit the particular kinematical properties of the VBS SSWW reaction [62]. The agreement of the input variables used to train the DNN models has been thoroughly checked in the CRs introduced at the beginning of this section. First, there are the transverse masses

$$m_{1\mathrm{T}}^2 = \left(\sqrt{m_{\tau\ell}^2 + p_{\mathrm{T}}^{\tau\ell\,2}} + p_{\mathrm{T}}^{\mathrm{miss}}\right)^2 - |\vec{p}_{\mathrm{T}}^{\,\tau\ell} + \vec{p}_{\mathrm{T}}^{\,\mathrm{miss}}|^2, \text{ and} \tag{4}$$

$$m_{\circ 1}^2 = \left(p_{\mathrm{T}}^{\tau} + p_{\mathrm{T}}^{\ell} + p_{\mathrm{T}}^{\mathrm{miss}}\right)^2 - |\vec{p}_{\mathrm{T}}^{\,\tau} + \vec{p}_{\mathrm{T}}^{\,\ell} + \vec{p}_{\mathrm{T}}^{\,\mathrm{miss}}|^2. \tag{5}$$

The variable $m_{1\mathrm{T}}$ is the transverse mass of the $\tau\ell$ system with $p_{\mathrm{T}}^{\mathrm{miss}}$. For the second quantity, $m_{\circ 1}$, the τ, ℓ momenta, and $p_{\mathrm{T}}^{\mathrm{miss}}$ are treated as if coming from a system with a null invariant mass when calculating the transverse mass of the three objects. These two variables are a proxy for the energy of the scattering W boson pair, as well as for the angular distribution of the decay objects coming from that pair. With these quantities it is possible to access direct information on the process of interest for this study, more complete than the invariant mass of the VBS jet pair and the p_{T} of the leptons. In this way, it is possible to enhance the discrimination of the SSWW VBS signal processes against the background, especially when investigating the sensitivity to EFT contributions, as shown for $m_{\circ 1}$ in Fig. 3. The three transverse masses introduced so far are among the most important features for all of the DNNs.

Furthermore, the transverse masses $m_{\mathrm{T}}(\tau_{\mathrm{h}}, \vec{p}_{\mathrm{T}}^{\,\mathrm{miss}})$ and $m_{\mathrm{T}}(\ell + \tau_{\mathrm{h}}, \vec{p}_{\mathrm{T}}^{\,\mathrm{miss}})$, defined similarly to $m_{\mathrm{T}}(\ell, \vec{p}_{\mathrm{T}}^{\,\mathrm{miss}})$ in Eq. (3), are introduced. Next, we define the event Zeppenfeld variable [63]:

$$z_{\mathrm{event}} = \frac{1}{2}\frac{\eta_\ell - |\frac{\eta_{j_1}+\eta_{j_2}}{2}|}{\eta_{j_1} - \eta_{j_2}} + \frac{1}{2}\frac{\eta_{\tau_{\mathrm{h}}} - |\frac{\eta_{j_1}+\eta_{j_2}}{2}|}{\eta_{j_1} - \eta_{j_2}}, \tag{6}$$

introduced to exploit the centrality of the leptons in the VBS processes with respect to the scattered VBS jets j_1, j_2. Finally we add the component $p_{\mathrm{T},1j}^{\mathrm{rel}}$ of the ℓ or τ_{h} momentum $\vec{p}_1$ perpendicular to the momentum $\vec{p}_j$ of VBS jet j:

$$p_{\mathrm{T},1j}^{\mathrm{rel}} = \frac{|\vec{p}_1 \times \vec{p}_j|}{|\vec{p}_j|}. \tag{7}$$

This variable evaluates how close a lepton is to the flight direction of a jet. For VBS processes, this quantity is expected to be distributed towards values larger than for the other processes, since the light lepton and the τ_{h} produced by the scattered W bosons are far from the VBS jets.

The pre-fit $m_{\circ 1}$ distributions in the SRs for the electron and muon final states are shown in Fig. 3.

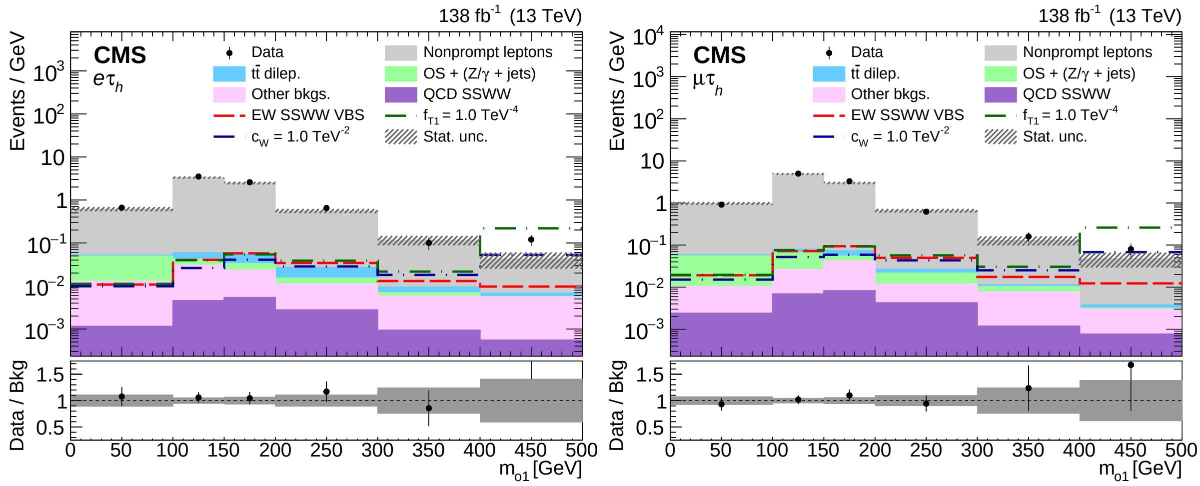

Figure 3: Distributions in $m_{\circ 1}$ transverse mass for the data and the pre-fit background prediction for the (left) $e\tau_h$ and (right) $\mu\tau_h$ SRs. The stacked filled histograms show the background components, and the overflow count is included in the last bin. The expectations for the EW SSWW signal, the $\mathcal{O}_W$ dim-6 operator with $c_W = 1\,\text{TeV}^{-2}$, and the $\mathcal{Q}_{T1}$ dim-8 operator with $f_{T1} = 1\,\text{TeV}^{-4}$ are shown by the solid red, blue, and green lines, respectively. For the latter two, the interference with SM and pure EFT contributions are summed together with the SM contribution. The hatched error band shows the bin-by-bin statistical uncertainty. The lower panels show the ratio of data to the total background prediction, with statistical uncertainties indicated by error bars and hatched shading, respectively. In all the panels, the vertical bars represent the statistical uncertainty assigned to the observed number of events.

For the measurement of the SM VBS processes under investigation, the statistical analysis is implemented with an ML fit to extract the signal strength, defined as the ratio of the signal yield observed to that predicted by the model, taking the asymptotic limit of Wilks's theorem [64]. The ML fit is implemented with the CMS statistical analysis tool COMBINE [65], which is based on the ROOFIT [66] and ROOSTATS [67] frameworks. To validate the results obtained by relying on the asymptotic limit, we perform the same measurement by generating pseudo-experiments for the signal and the background, taking into account their statistical fluctuations. The outcomes from the pseudo-experiments are consistent with the ones returned by applying Wilks's theorem, and in the following the latter are presented. Data yields in both SRs and CRs are incorporated in the likelihood via Poisson probability density functions. The inputs to the fit are the distributions in the DNN output of the data, the signal, and the backgrounds estimated as described above. The distributions in the SRs and CRs are affected by common sources of systematic uncertainty, described in the next section, and thus their expectations are treated as correlated in the fit.

The statistical analysis for the investigation of the EFT contributions in the VBS processes of interest is also based on an ML fit, considering that the expected number of events N_{exp} inherits the quadratic dependence on the EFT Wilson coefficients from the scattering amplitude $|\mathcal{A}_{\text{BSM}}|$ reported in Eq. (2). When the contribution of a single EFT dim-6 (with c_i Wilson coefficient) or dim-8 (with f_α Wilson coefficient) operator is considered, and all the others are set to null

Table 2: List of the input variables for the three DNN models developed in this study. The check mark indicates that the variable is included in the DNN model identified in the column header.

Input variable	SM DNN	dim-6 DNN	dim-8 DNN
τ_{h} p_{T}	✓	✓	✓
ℓ p_{T}	✓	✓	✓
τ_{h} η		✓	
ℓ η		✓	
leading VBS jet p_{T}	✓	✓	✓
subleading VBS jet p_{T}	✓	✓	✓
leading VBS jet mass		✓	✓
subleading VBS jet mass		✓	✓
VBS jet pair $\Delta\phi$		✓	
m_{jj}	✓	✓	
m_{1T}	✓	✓	✓
$m_{\circ 1}$	✓	✓	✓
$m_{\mathrm{T}}(\tau_{\mathrm{h}}, \vec{p}_{\mathrm{T}}^{\mathrm{miss}})$			✓
$m_{\mathrm{T}}(\ell, \vec{p}_{\mathrm{T}}^{\mathrm{miss}})$	✓	✓	✓
$m_{\mathrm{T}}(\ell + \tau_{\mathrm{h}}, \vec{p}_{\mathrm{T}}^{\mathrm{miss}})$			✓
$p_{\mathrm{T}}^{\mathrm{rel}}(\ell, j_1)$		✓	
$p_{\mathrm{T}}^{\mathrm{rel}}(\ell, j_2)$		✓	
$p_{\mathrm{T}}^{\mathrm{rel}}(\tau_{\mathrm{h}}, j_1)$		✓	
$p_{\mathrm{T}}^{\mathrm{rel}}(\tau_{\mathrm{h}}, j_2)$		✓	
$\Delta\phi(\ell, j_1)$		✓	
$\Delta\phi(\ell, j_2)$		✓	
$\Delta\phi(\tau_{\mathrm{h}}, j_1)$		✓	
$\Delta\phi(\tau_{\mathrm{h}}, j_2)$		✓	
$p_{\mathrm{T,\,leading}\ \tau_{\mathrm{h}}\ \mathrm{track}} / p_{\mathrm{T},\,\tau_{\mathrm{h}}}$	✓	✓	
z_{event}		✓	

values, the expected number of events can be written as follows:

$$N^{i}_{\text{exp}} = N_{\text{SM}} + \frac{c_i}{\Lambda^2} N^{i}_{\text{Lin}} + \frac{c_i^2}{\Lambda^4} N^{i}_{\text{Quad}}, \tag{8}$$

$$N^{\alpha}_{\text{exp}} = N_{\text{SM}} + \frac{f_\alpha}{\Lambda^4} N^{\alpha}_{\text{Lin}} + \frac{f_\alpha^2}{\Lambda^8} N^{\alpha}_{\text{Quad}}, \tag{9}$$

where N_{SM} stands for the contribution from the SM processes, N_{Lin} for the one from the interference of the considered EFT operator with the SM VBS processes, and N_{Quad} for the pure term produced by the specific operator. In the following, this fit setup will be referred to as a 1D dim-6 or dim-8 EFT study, respectively. When two EFT dim-6 operators with Wilson coefficients c_i, c_j are considered active, and all the other ones are set as negligible, the same quantity reads:

$$N^{i,j}_{\text{exp}} = N_{\text{SM}} + \sum_{k=i,j} \left(\frac{c_k}{\Lambda^2} N^{k}_{\text{Lin}} + \frac{c_k^2}{\Lambda^4} N^{k}_{\text{Quad}} \right) + \frac{c_i c_j}{\Lambda^4} N^{ij}_{\text{Cross}}, \tag{10}$$

where N_{Cross} represents the interference between the two EFT operators under study. This fit setup will be called a two-dimensional (2D) same-dimension EFT study in the rest of this paper. Finally, when considering one EFT dim-6 and one dim-8 operator with Wilson coefficients c_i, f_α to be active, the expected number of events becomes:

$$N^{i,\alpha}_{\text{exp}} = N_{\text{SM}} + \frac{c_i}{\Lambda^2} N^{i}_{\text{Lin}} + \frac{c_i^2}{\Lambda^4} N^{i}_{\text{Quad}} + \frac{f_\alpha}{\Lambda^4} N^{\alpha}_{\text{Lin}} + \frac{f_\alpha^2}{\Lambda^8} N^{\alpha}_{\text{Quad}}. \tag{11}$$

This fit setup will be referred to as a 2D different-dimension EFT study. It neglects the contributions due to the possible interference between the dim-6 and the dim-8 operator, for which there are no clear theoretical predictions.

6 Systematic uncertainties

Systematic uncertainties in the signal and background yields are introduced as nuisance parameters in the ML fit, both for the measurement of the VBS SSWW processes and for the EFT investigations.

The uncertainties determined by the CMS luminosity monitoring are partially correlated among the data sets [68–70], resulting in overall uncertainties of 1.2, 2.3, and 2.5% for the 2016, 2017, and 2018 integrated luminosities, respectively. This uncertainty affects only the integrated yields, not the shapes of the distributions.

Uncertainties at the matrix-element level, which impact both the normalization and shape of the background and signal processes, are evaluated through separate variations of the renormalization and factorization scales. Specifically, the renormalization scale is varied by a factor of 2 (or 0.5) while keeping the factorization scale fixed, and vice versa. The resulting uncertainties are then combined by taking the envelope of these variations relative to the nominal expectation [71]. These uncertainties are considered uncorrelated across different process categories but are correlated across the data-taking years.

The MC samples are generated using a default PDF set, as mentioned in Section 3, and event weights corresponding to the 100 PDF alternative set members are also stored, evaluated with the MadGraph5_aMC@NLO reweighting technique introduced in Section 3. These are used to evaluate the PDF systematic uncertainties according to the procedure recommended by the PDF4LHC group [72], which is based on the same strategy explained in the previous paragraph. They are correlated among the data-taking years and processes.

Among the possible theoretical uncertainties affecting MC simulations are those related to the QCD-induced parton-shower modeling. These are divided into initial-state radiation (ISR) and final-state radiation (FSR) and are considered correlated among the data-taking years and processes.

Uncertainties in b tagging and mistagging data-to-simulation scale factors (SFs) are applied to reproduce the corresponding efficiencies measured in the data, and implemented in the ML fit as correlated among the data-taking years.

Systematic uncertainties related to the pileup modeling are introduced as a $\pm4.6\%$ variation in the total inelastic cross section of 69.2 mb that is used to estimate the data pileup distributions [73]. They are correlated among the data-taking years.

The impact of the uncertainty in the trigger efficiency measurement is estimated by varying the SFs within their uncertainties separately for each data-taking year and final state. This uncertainty is treated as uncorrelated among data-taking years.

In 2016 and 2017, a portion of trigger primitives in the ECAL was associated with the wrong bunch crossing, leading to a trigger mistiming effect and a nonnegligible decrease in the trigger efficiency that is not modeled in the simulated samples [74]. Events have been corrected for this effect with a per-event weight, and the corresponding uncertainties have been propagated throughout the analysis chain. They are correlated among the data-taking years.

In simulated events, reconstructed four-momenta of all of the jets are simultaneously varied according to the η- and p_{T}-dependent uncertainties in the jet energy scale; they are correlated among data-taking years. These variations are then propagated to the $\vec{p}_{\mathrm{T}}^{\,\mathrm{miss}}$. Moreover, to properly evaluate the systematic effect coming from differences in the jet energy resolution between data and simulations, smearing is also applied to the latter by varying the jet resolutions according to their uncertainties; they are uncorrelated among the data-taking years [75]. Because of the high efficiency of the jet quality requirements, no SFs or associated uncertainties for those are applied.

Systematics related to uncertainties affecting unclustered energy in the calorimeters are included in the fit and correlated among data-taking years.

Systematic uncertainties due to SFs used to match the efficiencies in light lepton reconstruction, identification, isolation, and energy scale and resolution as measured in the MC samples with those observed in data, are evaluated by varying the corresponding event weights by the SF uncertainty. They are uncorrelated over the data-taking years.

For the uncertainty arising from charge sign misreconstruction in the $\mathrm{e}\tau_{\mathrm{h}}$ channel we assign a uniform uncertainty of 15% to the distributions of the background processes, consistent with the data-background agreement observed in the OS CR.

Statistical uncertainties related to the τ lepton identification SFs and the corrections to their energy scale and resolution [57] induce a systematic effect on the expected signal and background distributions. Their impact is evaluated following a procedure similar to the one applied for light-lepton systematic uncertainties. They are uncorrelated among the data-taking years.

The LO to NLO corrections to the VBS signal come with statistical uncertainties that are propagated to the fit [31–33].

For the signal and background processes estimated from simulation, the precision of the modeling is limited by the event count in the MC samples. The corresponding statistical uncertainties are therefore taken as systematic uncertainties applied to each bin of the corresponding distribution, according to the lite Barlow-Beeston method [76].

The estimate of the nonprompt background is affected by the statistical uncertainties of the auxiliary regions used to measure the transfer factors. This uncertainty is propagated by the lite Barlow-Beeston method [76]. We assign a further 30% normalization uncertainty based on a closure test performed in the nonprompt CR. This uncertainty is treated as correlated among the data-taking years.

In the following, we collectively refer to the statistical uncertainties assigned to the backgrounds, extracted from data CRs or from simulation, as background statistical. It represents the dominant source of overall uncertainty.

The impacts of the systematic uncertainties in the signal strength, as extracted from the ML fit, are summarized in Table 3.

Table 3: The impact of each systematic uncertainty, together with the impact of the data statistical uncertainty, on the signal strength μ, as extracted from the fit to measure the SM SSWW VBS signal with the DNN output distributions. Upper and lower uncertainties are given for the various sources.

Uncertainty source	$+\Delta\mu$	$-\Delta\mu$
Theory (PDF, scales, ISR, FSR)	+0.16	−0.10
Nonprompt background estimation	+0.13	−0.12
$t\bar{t}$ normalization	+0.051	−0.023
Trigger mistiming	+0.105	−0.059
Luminosity	+0.079	−0.092
b tagging and mistagging	+0.007	−0.004
Jet energy scale, resolution, and identification	+0.079	−0.097
Pileup	+0.15	−0.16
LO-to-NLO VBS corrections	+0.043	−0.025
Unclustered energy	+0.003	−0.010
τ_h energy scale and identification	+0.15	−0.15
Charge misidentification	+0.005	−0.010
Lepton reconstruction, identification, and isolation	+0.005	−0.024
Background statistical	+0.32	−0.32
Total systematic	+0.34	−0.30
Data statistical	+0.52	−0.48
Total	+0.62	−0.56

7 Measurement of the SM SSWW VBS processes

We extract values of the signal strength and the statistical significance from the fit of the SM SSWW VBS signal, with two separate interpretations. As the primary interpretation, we measure the purely EW signal strength keeping the QCD SSWW production contribution fixed to the SM prediction. In the second interpretation, we measure the signal strength treating as signal the combined EW and QCD SSWW processes, fixing the ratio between the two contributions to the SM value. For the primary result of the EW signal strength measurement, the DNN output distributions of the SR and the $t\bar{t}$ and OS CRs are shown in Fig. 4 for both the electron and muon flavors.

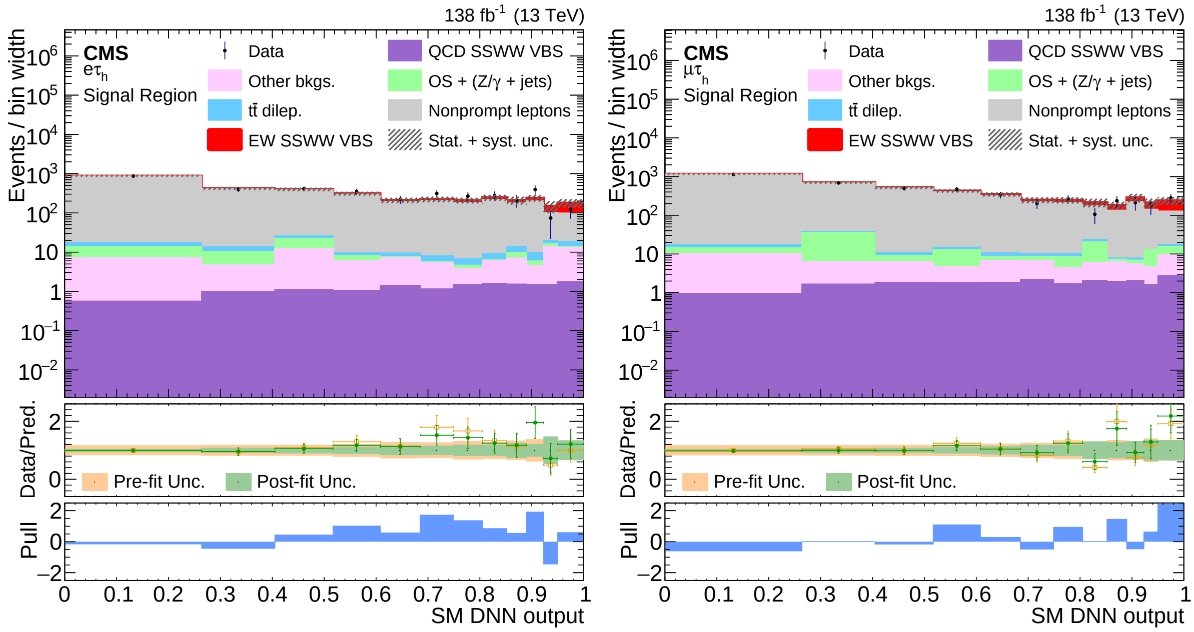

Figure 4: Distribution of the DNN output for the (left) $e\tau_h$ and (right) $\mu\tau_h$ SR. The data points are overlaid on the post-fit background (stacked histograms). The overflow is included in the last bin. The middle panels show ratios of the data to the pre-fit background prediction and post-fit background yield in yellow and green, respectively. The corresponding colored bands indicate the systematic component of the uncertainty. The lower panels show the distributions of the pulls, defined in the text. The blue shading in these panels represents the total uncertainty in the signal and background estimates. In all the panels, the vertical bars represent the statistical uncertainty assigned to the observed number of events.

In Fig. 4, the data are compared with the background estimated before (pre-fit) and after (post-fit) the simultaneous fit of the SRs and CRs. The pulls shown in the lower panels are defined, for each bin, as

$$\text{Pull} = \frac{n_{\text{data}} - n_{\text{post-fit}}}{\sqrt{\sigma^2_{\text{data}} - \sigma^2_{\text{post-fit}}}}, \qquad (12)$$

where n_{data} and $n_{\text{post-fit}}$ are respectively measured event numbers and post-fit background predictions, and σ_{data} and $\sigma_{\text{post-fit}}$ are their corresponding uncertainties. The quadratic difference of the uncertainties appearing in the denominator is taken to account for the correlation between the data and the post-fit prediction. The observed (expected) EW signal strength is $1.44^{+0.63}_{-0.56}$ ($1.00^{+0.60}_{-0.53}$), corresponding to a signal significance of 2.7 (1.9) standard deviations. The simultaneous measurement of the EW and QCD-associated SSWW production results in an observed (expected) signal strength equal to $1.43^{+0.60}_{-0.54}$ ($1.00^{+0.57}_{-0.51}$), with a significance of 2.9 (2.0) standard deviations. The largest contribution to the overall uncertainty is the statistical uncertainty of the data, as reported in Table 3.

Tabulated results are provided in the HEPData record for this analysis [77].

8 Effective field theory interpretation

The sensitivity of the measurement to the dim-6 and dim-8 EFT operators, considered one at a time, is estimated from a likelihood scan performed by varying the corresponding Wilson coefficients as they appear in the quadratic parametrization of the signal yields given by Eqs. (8) and (9). For this part of the study, we use the distributions of the dim-6 and dim-8 DNN outputs, respectively. No significant deviations from the SM predictions are observed. The 68 and 95% confidence intervals on the Wilson coefficients are extracted from the scan and reported in Table 4. Although CMS and ATLAS have published dim-8 VBS analysis [12], these represent the first limits set on EFT dim-6 operator contributions in VBS processes.

Table 4: Observed and expected 68 and 95% 1D confidence level (CL) intervals on the Wilson coefficients associated with the EFT dim-6 and dim-8 operators considered. The results reported here are obtained by fixing the Wilson coefficients other than the one of interest to their SM values in the fit procedure.

Wilson coefficient		68% CL interval(s)		95% CL interval	
		Observed	Expected	Observed	Expected
dim-6	$c_{ll}^{(1)}/\Lambda^2$	$[-11.6, 0.045]$	$[-12.9, -8.03] \cup [-2.95, 1.91]$	$[-13.5, 2.11]$	$[-14.6, 3.53]$
	$c_{qq}^{(1)}/\Lambda^2$	$[-0.341, 0.416]$	$[-0.501, 0.576]$	$[-0.605, 0.681]$	$[-0.742, 0.818]$
	c_W/Λ^2	$[-0.513, 0.481]$	$[-0.681, 0.669]$	$[-0.842, 0.818]$	$[-0.987, 0.974]$
	c_{HW}/Λ^2	$[-5.48, 4.31]$	$[-7.00, 6.09]$	$[-8.68, 7.60]$	$[-9.99, 9.05]$
	c_{HWB}/Λ^2	$[-30.7, 89.2]$	$[-41.7, 69.6]$	$[-49.7, 110]$	$[-66.6, 96.4]$
	$c_{H\Box}/\Lambda^2$	$[-12.0, 14.0]$	$[-16.6, 18.1]$	$[-20.9, 22.7]$	$[-24.7, 26.3]$
	c_{HD}/Λ^2	$[-15.3, 31.5]$	$[-24.6, 34.7]$	$[-31.4, 45.5]$	$[-38.2, 48.8]$
	$c_{Hl}^{(1)}/\Lambda^2$	$[-38.2, 39.5]$	$[-28.8, 29.9]$	$[-69.3, 68.3]$	$[-49.4, 49.7]$
	$c_{Hl}^{(3)}/\Lambda^2$	$[-0.045, 8.58]$	$[-1.43, 2.23] \cup [5.88, 9.54]$	$[-1.59, 9.94]$	$[-2.64, 10.8]$
	$c_{Hq}^{(1)}/\Lambda^2$	$[-3.27, 3.44]$	$[-4.53, 4.42]$	$[-5.55, 5.60]$	$[-6.56, 6.44]$
	$c_{Hq}^{(3)}/\Lambda^2$	$[-1.88, 0.705]$	$[-2.39, 1.37]$	$[-2.82, 1.61]$	$[-3.24, 2.16]$
dim-8	f_{T0}/Λ^4	$[-0.774, 0.842]$	$[-1.02, 1.08]$	$[-1.32, 1.38]$	$[-1.52, 1.58]$
	f_{T1}/Λ^4	$[-0.319, 0.381]$	$[-0.426, 0.480]$	$[-0.552, 0.613]$	$[-0.640, 0.695]$
	f_{T2}/Λ^4	$[-0.851, 1.12]$	$[-1.15, 1.37]$	$[-1.51, 1.76]$	$[-1.75, 1.98]$
	f_{M0}/Λ^4	$[-8.07, 7.70]$	$[-9.89, 9.74]$	$[-13.1, 12.8]$	$[-14.6, 14.5]$
	f_{M1}/Λ^4	$[-9.54, 11.15]$	$[-12.5, 13.3]$	$[-16.4, 17.7]$	$[-18.7, 19.6]$
	f_{M7}/Λ^4	$[-17.6, 15.3]$	$[-20.3, 19.2]$	$[-27.6, 25.8]$	$[-29.9, 28.8]$
	f_{S0}/Λ^4	$[-9.60, 9.82]$	$[-11.6, 12.0]$	$[-15.9, 16.1]$	$[-17.4, 17.9]$
	f_{S1}/Λ^4	$[-40.9, 41.3]$	$[-37.4, 38.8]$	$[-60.9, 61.8]$	$[-57.2, 58.6]$
	f_{S2}/Λ^4	$[-40.9, 41.3]$	$[-37.4, 38.8]$	$[-60.9, 61.8]$	$[-57.2, 58.6]$

In addition, a 2D likelihood scan is performed over pairs of Wilson coefficients as they appear in Eqs. (10) and (11), exploiting the distributions of $m_{\circ 1}$, which we find to be the most sensitive variable to EFT effects among the kinematic quantities considered. For the same-dimension fits, we consider pairs of EFT operators that both modify either the WW $\rightarrow$ WW amplitude or the W pairing with fermions. For the different-dimension fits, we consider pairs that modify the WW $\rightarrow$ WW amplitude. The operators in these pairs impact the scattering amplitude with similar magnitudes in terms of linear and quadratic contributions.

The results are reported in Figs. 5 and 6. For the same-dimension pairs shown in the upper two rows of Fig. 5, combining the effects of two operators leads to a broadening of the 68 and 95% CL intervals extracted with the corresponding one-dimensional fit to the $m_{\circ 1}$ distributions, an effect that is more pronounced for the operators to which this analysis is less sensitive. In general, the contours have an elliptical shape with correlation effects driven by the interference between the operators considered in the pairs, particularly for the mixed dim-6 operators, as shown in the lower row of Fig. 5. The results for the $\mathcal{O}_{HWB}$, $\mathcal{O}_{H\Box}$ operator pair (reported at the middle right of Fig. 5) have some peculiarities, ascribable to the fact that these terms generate very similar interference with the SM contribution when the corresponding Wilson coefficients have unity values. For the expected contours, this is translated into a negative linear correlation that tilts the axes of the ellipses; for the observed contours, the correlation effect is enhanced by fluctuations in data that both operators can account for.

For the different-dimension pairs, the results show that the addition of the linear and quadratic dim-8 contributions to the corresponding ones for a given dim-6 operator leads to a slight broadening of the one-dimensional 68 and 95% intervals for the dim-6 operators, independently of the specific dim-8 operator considered in the pair. The same broadening effect can be observed for the dim-8 Wilson coefficients. However, the relative impact of this broadening effect on the dim-6 Wilson coefficients is not consistent among all of them, being more pronounced when the dim-6 and dim-8 contributions are comparable within a few orders of magnitude. The latter fact also has an impact on the shape of the contours, which is more circular for the pairs with comparable dim-6 and dim-8 effects, and more rectangular when dim-8 contributions are negligible with respect to the dim-6 terms. In addition, the contour does not show evidence of linear correlations, as the possible interference between the dim-6 and the dim-8 operators in the pair is neglected in this study. These considerations lead to the conclusion that, within the EFT framework, the one-dimensional constraints on a Wilson coefficient associated with a given operator could be biased by neglect of the contributions of other operators arising in the same physical process and at the same or different power of Λ_{BSM}.

It is worth noting that the 2D EFT fits with two dim-6 operators represent the first results of this type for an analysis investigating VBS processes, and the 2D EFT fits with one dim-6 and one dim-8 operator represent the first results ever for combinations of different-dimension EFT operators in the same physics processes.

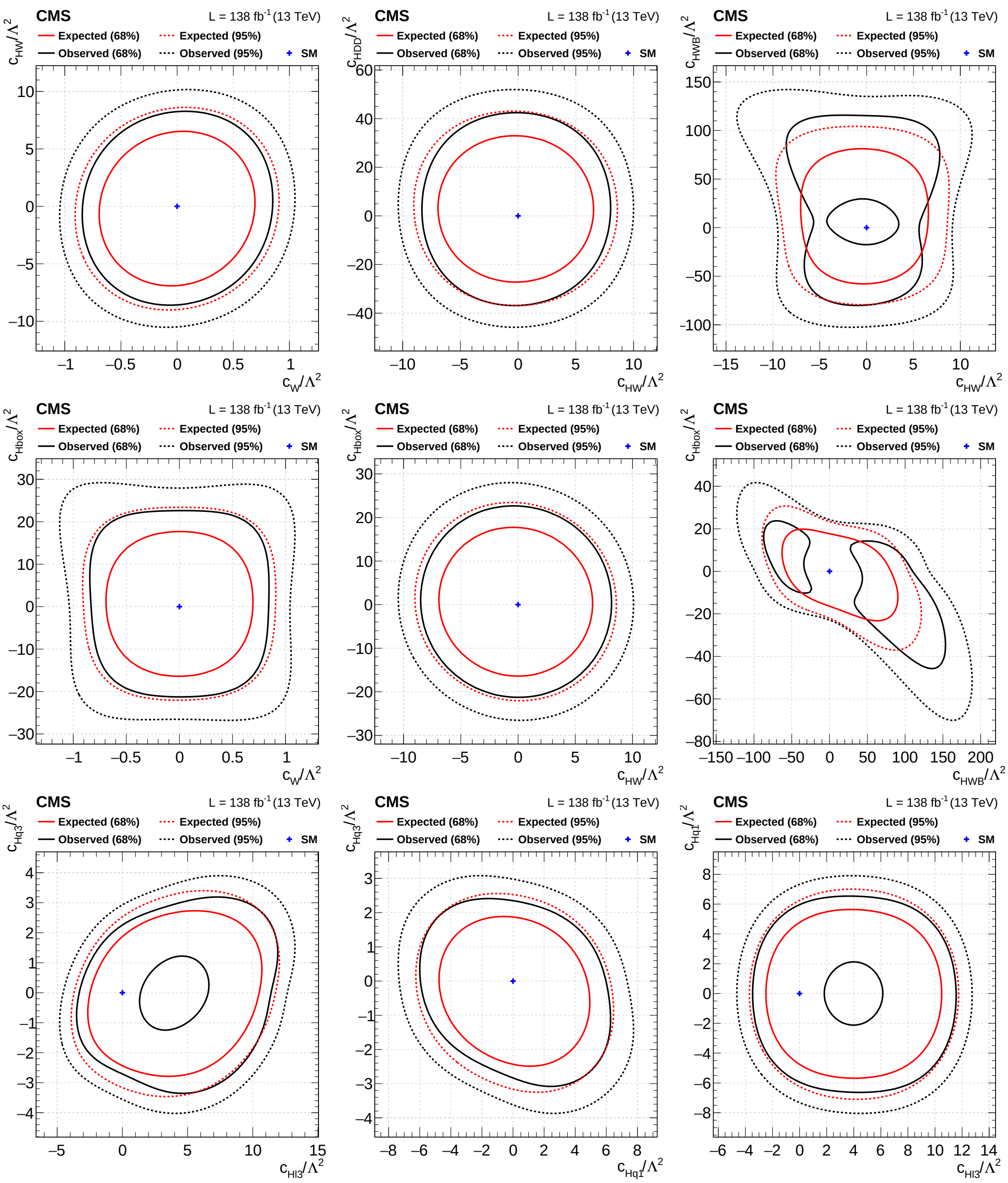

Figure 5: Observed (black) and expected (red) 68 (solid) and 95% (dashed) CL contours for $-2\ln\Delta\mathcal{L}$ as functions of the reported dim-6 bosonic (upper two rows) and mixed (lower row) Wilson coefficient pairs. When there are two contours for the same CL value, the constrained set of Wilson coefficient values is represented by the area between the two of them if they are concentric, otherwise it consists of the internal areas of the contours.

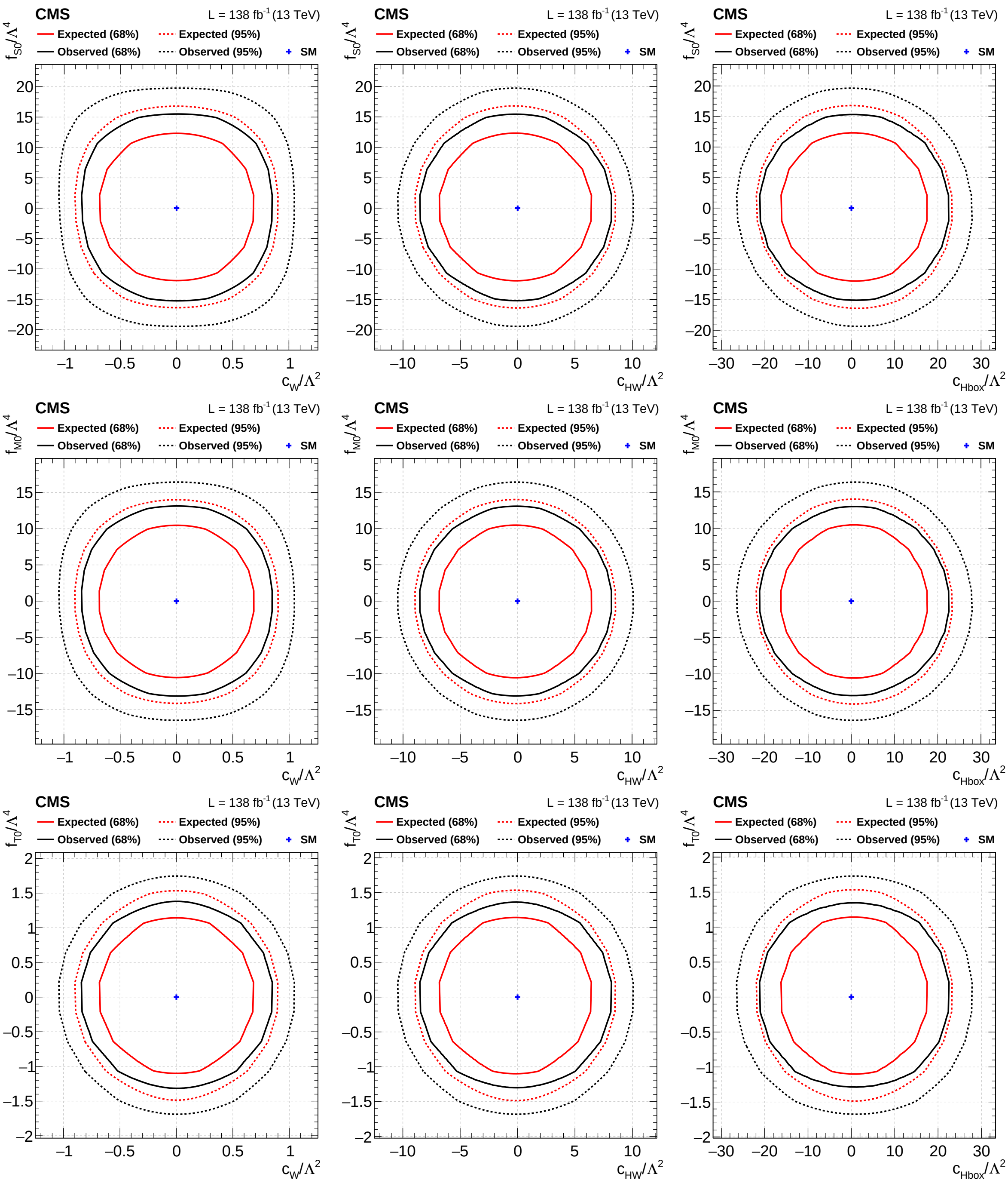

Figure 6: Observed (black) and expected (red) 68 (solid) and 95% (dashed) CL contours for $-2\ln\Delta\mathcal{L}$ as functions of the reported (dim-6, dim-8) Wilson coefficient pairs.

9 Summary

Electroweak (EW) production of a same-sign W boson pair, with a hadronically decaying τ lepton in the final state, is investigated for the first time, together with an interpretation of possible deviations from the standard model expectations in terms of effective field theory (EFT) operators of dimension 6 and 8. The analysis is performed with a sample of proton-proton collisions at $\sqrt{s} = 13\,\text{TeV}$ recorded by the CMS experiment at the CERN LHC in 2016–2018, corresponding to an integrated luminosity of $138\,\text{fb}^{-1}$. Events are selected with the requirement of one τ lepton together with one light lepton (e or μ) of the same sign, missing transverse momentum, and two jets with large pseudorapidity separation and large dijet invariant mass. Deep neural network algorithms are employed to discriminate different types of signal events from the main backgrounds, significantly boosting the sensitivity of the search.

The amplitude for same-sign WW production includes terms that account for strong interactions between partons with W boson radiation. A small fraction of these QCD-mediated events falls within the acceptance of the search. The measured cross section for EW same-sign WW scattering, extracted with the QCD-mediated amplitudes fixed to the standard model (SM) expectations, is $1.44^{+0.63}_{-0.56}$ times the SM prediction. The observed (expected) significance of the EW signal is 2.7 (1.9) standard deviations. A measurement of the combined EW and residual QCD-mediated contributions yields an observed (expected) significance of 2.9 (2.0) standard deviations.

Also presented are the first limits in vector boson scattering on dimension-6 EFT operator contributions, including both one operator and two operators active at the same time. This is the first study of the combined effects of EFT operators with different dimensions, showing that focusing on one dimensionality can lead to an overestimate of the sensitivity to the corresponding EFT operator class, and that the contributions of terms combining operators with different dimensions should not be neglected.

Acknowledgments

We congratulate our colleagues in the CERN accelerator departments for the excellent performance of the LHC and thank the technical and administrative staffs at CERN and at other CMS institutes for their contributions to the success of the CMS effort. In addition, we gratefully acknowledge the computing centers and personnel of the Worldwide LHC Computing Grid and other centers for delivering so effectively the computing infrastructure essential to our analyses. Finally, we acknowledge the enduring support for the construction and operation of the LHC, the CMS detector, and the supporting computing infrastructure provided by the following funding agencies: SC (Armenia), BMBWF and FWF (Austria); FNRS and FWO (Belgium); CNPq, CAPES, FAPERJ, FAPERGS, and FAPESP (Brazil); MES and BNSF (Bulgaria); CERN; CAS, MoST, and NSFC (China); MINCIENCIAS (Colombia); MSES and CSF (Croatia); RIF (Cyprus); SENESCYT (Ecuador); ERC PRG, RVTT3 and MoER TK202 (Estonia); Academy of Finland, MEC, and HIP (Finland); CEA and CNRS/IN2P3 (France); SRNSF (Georgia); BMBF, DFG, and HGF (Germany); GSRI (Greece); NKFIH (Hungary); DAE and DST (India); IPM (Iran); SFI (Ireland); INFN (Italy); MSIP and NRF (Republic of Korea); MES (Latvia); LMTLT (Lithuania); MOE and UM (Malaysia); BUAP, CINVESTAV, CONACYT, LNS, SEP, and UASLP-FAI (Mexico); MOS (Montenegro); MBIE (New Zealand); PAEC (Pakistan); MES and NSC (Poland); FCT (Portugal); MESTD (Serbia); MCIN/AEI and PCTI (Spain); MOSTR (Sri Lanka); Swiss Funding Agencies (Switzerland); MST (Taipei); MHESI and NSTDA (Thailand); TUBITAK and TENMAK (Turkey); NASU (Ukraine); STFC (United Kingdom); DOE and NSF

(USA).

Individuals have received support from the Marie-Curie program and the European Research Council and Horizon 2020 Grant, contract Nos. 675440, 724704, 752730, 758316, 765710, 824093, 101115353, 101002207, and COST Action CA16108 (European Union); the Leventis Foundation; the Alfred P. Sloan Foundation; the Alexander von Humboldt Foundation; the Science Committee, project no. 22rl-037 (Armenia); the Belgian Federal Science Policy Office; the Fonds pour la Formation à la Recherche dans l'Industrie et dans l'Agriculture (FRIA-Belgium); the F.R.S.-FNRS and FWO (Belgium) under the "Excellence of Science – EOS" – be.h project n. 30820817; the Beijing Municipal Science & Technology Commission, No. Z191100007219010 and Fundamental Research Funds for the Central Universities (China); the Ministry of Education, Youth and Sports (MEYS) of the Czech Republic; the Shota Rustaveli National Science Foundation, grant FR-22-985 (Georgia); the Deutsche Forschungsgemeinschaft (DFG), among others, under Germany's Excellence Strategy – EXC 2121 "Quantum Universe" – 390833306, and under project number 400140256 - GRK2497; the Hellenic Foundation for Research and Innovation (HFRI), Project Number 2288 (Greece); the Hungarian Academy of Sciences, the New National Excellence Program - ÚNKP, the NKFIH research grants K 131991, K 133046, K 138136, K 143460, K 143477, K 146913, K 146914, K 147048, 2020-2.2.1-ED-2021-00181, and TKP2021-NKTA-64 (Hungary); the Council of Science and Industrial Research, India; ICSC – National Research Center for High Performance Computing, Big Data and Quantum Computing and FAIR – Future Artificial Intelligence Research, funded by the NextGenerationEU program (Italy); the Latvian Council of Science; the Ministry of Education and Science, project no. 2022/WK/14, and the National Science Center, contracts Opus 2021/41/B/ST2/01369 and 2021/43/B/ST2/01552 (Poland); the Fundação para a Ciência e a Tecnologia, grant CEECIND/01334/2018 (Portugal); the National Priorities Research Program by Qatar National Research Fund; MCIN/AEI/10.13039/501100011033, ERDF "a way of making Europe", and the Programa Estatal de Fomento de la Investigación Científica y Técnica de Excelencia María de Maeztu, grant MDM-2017-0765 and Programa Severo Ochoa del Principado de Asturias (Spain); the Chulalongkorn Academic into Its 2nd Century Project Advancement Project, and the National Science, Research and Innovation Fund via the Program Management Unit for Human Resources & Institutional Development, Research and Innovation, grant B39G670016 (Thailand); the Kavli Foundation; the Nvidia Corporation; the SuperMicro Corporation; the Welch Foundation, contract C-1845; and the Weston Havens Foundation (USA).

References

[1] ATLAS and CMS Collaborations, "Measurements of the Higgs boson production and decay rates and constraints on its couplings from a combined ATLAS and CMS analysis of the LHC pp collision data at $\sqrt{s} = 7$ and 8 TeV", *JHEP* **08** (2016) 045, doi:10.1007/JHEP08(2016)045, arXiv:1606.02266.

[2] P. W. Higgs, "Broken symmetries, massless particles and gauge fields", *Phys. Lett.* **12** (1964) 132, doi:10.1016/0031-9163(64)91136-9.

[3] P. W. Higgs, "Broken symmetries and the masses of gauge bosons", *Phys. Rev. Lett.* **13** (1964) 508, doi:10.1103/PhysRevLett.13.508.

[4] F. Englert and R. Brout, "Broken symmetry and the mass of gauge vector mesons", *Phys. Rev. Lett.* **13** (1964) 321, doi:10.1103/PhysRevLett.13.321.

[5] J. Chang, K. Cheung, C.-T. Lu, and T.-C. Yuan, “WW scattering in the era of post-Higgs-boson discovery”, *Phys. Rev. D* **87** (2013) 093005, doi:10.1103/PhysRevD.87.093005, arXiv:1303.6335.

[6] W. Kilian, T. Ohl, J. Reuter, and M. Sekulla, “High-energy vector boson scattering after the Higgs boson discovery”, *Phys. Rev. D* **91** (2015) 96007, doi:10.1103/PhysRevD.91.096007, arXiv:1408.6207.

[7] C. Garcia-Garcia, M. Herrero, and R. A. Morales, “Unitarization effects in EFT predictions of WZ scattering at the LHC”, *Phys. Rev. D* **100** (2019) 096003, doi:10.1103/PhysRevD.100.096003, arXiv:1907.06668.

[8] ATLAS Collaboration, “Evidence for electroweak production of $W^{\pm}W^{\pm}$jj in pp collisions at $\sqrt{s} = 8$ TeV with the ATLAS Detector”, *Phys. Rev. Lett.* **113** (2014) 141803, doi:10.1103/PhysRevLett.113.141803, arXiv:1405.6241.

[9] CMS Collaboration, “Observation of electroweak production of same-sign W boson pairs in the two jet and two same-sign lepton final state in proton-proton collisions at $\sqrt{s} = 13$ TeV”, *Phys. Rev. Lett.* **120** (2018) 081801, doi:10.1103/PhysRevLett.120.081801, arXiv:1709.05822.

[10] CMS Collaboration, “Search for anomalous electroweak production of vector boson pairs in association with two jets in proton-proton collisions at 13 TeV”, *Phys. Lett. B* **798** (2019) 134985, doi:10.1016/j.physletb.2019.134985, arXiv:1905.07445.

[11] CMS Collaboration, “Evidence for electroweak production of four charged leptons and two jets in proton-proton collisions at $\sqrt{s}$ = 13 TeV”, *Phys. Lett. B* **812** (2021) 135992, doi:10.1016/j.physletb.2020.135992, arXiv:2008.07013.

[12] R. Covarelli, M. Pellen, and M. Zaro, “Vector-boson scattering at the LHC: unraveling the electroweak sector”, *Int. J. Mod. Phys. A* **36** (2021) 2130009, doi:10.1142/S0217751X2130009X, arXiv:2102.10991.

[13] S. Mantry, M. J. Ramsey-Musolf, and M. Trott, “New physics effects in Higgs decay to tau leptons”, *Phys. Lett. B* **660** (2008) 54, doi:10.1016/j.physletb.2007.12.021, arXiv:0707.3152.

[14] D. Rainwater, “Searching for the Higgs boson”, in *Theoretical Advanced Study Institute in Elementary Particle Physics: Exploring New Frontiers Using Colliders and Neutrinos*, p. 435. 2007. arXiv:hep-ph/0702124. doi:10.1142/9789812819260_0008.

[15] T. Plehn, D. L. Rainwater, and D. Zeppenfeld, “Determining the structure of Higgs couplings at the LHC”, *Phys. Rev. Lett.* **88** (2002) 051801, doi:10.1103/PhysRevLett.88.051801, arXiv:hep-ph/0105325.

[16] W. Buchmüller and D. Wyler, “Effective lagrangian analysis of new interactions and flavour conservation”, *Nucl. Phys. B* **268** (1986) 621, doi:10.1016/0550-3213(86)90262-2.

[17] B. Grzadkowski, M. Iskrzyński, M. Misiak, and J. Rosiek, “Dimension-six terms in the Standard Model Lagrangian”, *JHEP* **10** (2010) 085, doi:10.1007/JHEP10(2010)085, arXiv:1008.4884.

[18] ATLAS Collaboration, “Combined effective field theory interpretation of Higgs boson and weak boson production and decay with ATLAS data and electroweak precision observables”, Technical Report ATL-PHYS-PUB-2022-037, 2022.

[19] ATLAS Collaboration, “Top EFT summary plots April 2024”, Technical Report ATL-PHYS-PUB-2024-004, 2024.

[20] CMS Collaboration, “Measurement of $W^{\pm}\gamma$ differential cross sections in proton-proton collisions at $\sqrt{s}$ = 13 TeV and effective field theory constraints”, *Phys. Rev. D* **105** (2022) 052003, doi:10.1103/PhysRevD.105.052003, arXiv:2111.13948.

[21] CMS Collaboration, “Observation of $\gamma\gamma \to \tau\tau$ in proton-proton collisions and limits on the anomalous electromagnetic moments of the τ lepton”, *Rept. Prog. Phys.* **87** (2024) 107801, doi:10.1088/1361-6633/ad6fcb, arXiv:2406.03975.

[22] O. J. P. Éboli and M. C. Gonzalez-Garcia, “Classifying the bosonic quartic couplings”, *Phys. Rev. D* **93** (2016) 093013, doi:10.1103/PhysRevD.93.093013, arXiv:1604.03555.

[23] A. Falkowski et al., “Anomalous triple gauge couplings in the effective field theory approach at the LHC”, *JHEP* **02** (2017) 115, doi:10.1007/JHEP02(2017)115, arXiv:1609.06312.

[24] R. Bellan et al., “A sensitivity study of VBS and diboson WW to dimension-6 EFT operators at the LHC”, *JHEP* **05** (2022) 039, doi:10.1007/JHEP05(2022)039, arXiv:2108.03199.

[25] CMS Collaboration, “The CMS experiment at the CERN LHC”, *JINST* **3** (2008) 8004, doi:10.1088/1748-0221/3/08/S08004.

[26] CMS Collaboration, “Description and performance of track and primary-vertex reconstruction with the CMS tracker”, *JINST* **9** (2014) 10009, doi:10.1088/1748-0221/9/10/P10009, arXiv:1405.6569.

[27] CMS Collaboration, “The CMS phase-1 pixel detector upgrade”, *JINST* **16** (2021) P02027, doi:10.1088/1748-0221/16/02/P02027, arXiv:2012.14304.

[28] CMS Collaboration, “Track impact parameter resolution for the full pseudo rapidity coverage in the 2017 dataset with the CMS phase-1 pixel detector”, CMS Detector Performance Summary CMS-DP-2020-049, 2020.

[29] CMS Collaboration, “The CMS trigger system”, *JINST* **12** (2017) P01020, doi:10.1088/1748-0221/12/01/P01020, arXiv:1609.02366.

[30] J. Alwall et al., “The automated computation of tree-level and next-to-leading order differential cross sections, and their matching to parton shower simulations”, *JHEP* **07** (2014) 079, doi:10.1007/JHEP07(2014)079, arXiv:1405.0301.

[31] CMS Collaboration, “Measurements of production cross sections of WZ and same-sign WW boson pairs in association with two jets in proton-proton collisions at $\sqrt{s} = 13$ TeV”, *Phys. Lett. B* **809** (2020) 135710, doi:10.1016/j.physletb.2020.135710, arXiv:2005.01173.

[32] B. Biedermann, A. Denner, and M. Pellen, "Large electroweak corrections to vector-boson scattering at the Large Hadron Collider", *Phys. Rev. Lett.* **118** (2017) 261801, doi:10.1103/PhysRevLett.118.261801, arXiv:1611.02951.

[33] B. Biedermann, A. Denner, and M. Pellen, "Complete NLO corrections to W^+W^+ scattering and its irreducible background at the LHC", *JHEP* **10** (2017) 124, doi:10.1007/JHEP10(2017)124, arXiv:1708.00268.

[34] I. Brivio, "SMEFTsim 3.0 — a practical guide", *JHEP* **04** (2021) 073, doi:10.1007/JHEP04(2021)073, arXiv:2012.11343.

[35] I. Brivio, Y. Jiang, and M. Trott, "The SMEFTsim package, theory and tools", *JHEP* **12** (2017) 070, doi:10.1007/JHEP12(2017)070, arXiv:1709.06492.

[36] E. d. S. Almeida, O. J. P. Éboli, and M. C. Gonzalez–Garcia, "Unitarity constraints on anomalous quartic couplings", *Phys. Rev. D* **101** (2020) 113003, doi:10.1103/PhysRevD.101.113003, arXiv:2004.05174.

[37] O. Mattelaer, "On the maximal use of Monte Carlo samples: re-weighting events at NLO accuracy", *Eur. Phys. J. C* **76** (2016) 674, doi:10.1140/epjc/s10052-016-4533-7, arXiv:1607.00763.

[38] P. Nason, "A new method for combining NLO QCD with shower Monte Carlo algorithms", *JHEP* **11** (2004) 040, doi:10.1088/1126-6708/2004/11/040, arXiv:hep-ph/0409146.

[39] S. Frixione, P. Nason, and C. Oleari, "Matching NLO QCD computations with parton shower simulations: the POWHEG method", *JHEP* **11** (2007) 070, doi:10.1088/1126-6708/2007/11/070, arXiv:0709.2092.

[40] S. Alioli, P. Nason, C. Oleari, and E. Re, "A general framework for implementing NLO calculations in shower Monte Carlo programs: the POWHEG BOX", *JHEP* **06** (2010) 043, doi:10.1007/JHEP06(2010)043, arXiv:1002.2581.

[41] NNPDF Collaboration, "Parton distributions from high-precision collider data", *Eur. Phys. J. C* **77** (2017) 663, doi:10.1140/epjc/s10052-017-5199-5, arXiv:1706.00428.

[42] C. Bierlich et al., "A comprehensive guide to the physics and usage of PYTHIA 8.3", *SciPost Phys. Codeb.* **2022** (2022) 8, doi:10.21468/SciPostPhysCodeb.8, arXiv:2203.11601.

[43] CMS Collaboration, "Extraction and validation of a new set of CMS PYTHIA8 tunes from underlying-event measurements", *Eur. Phys. J. C* **80** (2020) 4, doi:10.1140/epjc/s10052-019-7499-4, arXiv:1903.12179.

[44] GEANT4 Collaboration, "GEANT4: A simulation toolkit", *Nucl. Instrum. Methods Phys. Res., A* **506** (2003) 250, doi:10.1016/S0168-9002(03)01368-8.

[45] CMS Collaboration, "Particle-flow reconstruction and global event description with the CMS detector", *JINST* **12** (2017) P10003, doi:10.1088/1748-0221/12/10/P10003, arXiv:1706.04965.

[46] M. Cacciari, G. P. Salam, and G. Soyez, "The anti-k_T jet clustering algorithm", *JHEP* **04** (2008) 063, doi:10.1088/1126-6708/2008/04/063, arXiv:0802.1189.

[47] M. Cacciari, G. P. Salam, and G. Soyez, "FastJet user manual", *Eur. Phys. J. C* **72** (2012) 1896, doi:10.1140/epjc/s10052-012-1896-2, arXiv:1111.6097.

[48] M. Cacciari and G. P. Salam, "Pileup subtraction using jet areas", *Phys. Lett. B* **659** (2008) 119, doi:10.1016/j.physletb.2007.09.077, arXiv:0707.1378.

[49] CMS Collaboration, "Jet performance in pp collisions at $\sqrt{s}$ = 7 TeV", CMS Physics Analysis Summary CMS-PAS-JME-10-003, 2010.

[50] CMS Collaboration, "Jet algorithms performance in 13 TeV data", CMS Physics Analysis Summary CMS-PAS-JME-16-003, 2017.

[51] CMS Collaboration, "Technical proposal for the Phase-II upgrade of the Compact Muon Solenoid", CMS Technical Proposal CERN-LHCC-2015-010, CMS-TDR-15-02, 2015.

[52] E. Bols et al., "Jet flavour classification using DeepJet", *JINST* **15** (2020) P12012, doi:10.1088/1748-0221/15/12/P12012, arXiv:2008.10519.

[53] CMS Collaboration, "Identification of heavy-flavour jets with the CMS detector in pp collisions at 13 TeV", *JINST* **13** (2018) P05011, doi:10.1088/1748-0221/13/05/P05011, arXiv:1712.07158.

[54] CMS Collaboration, "Measurement of the single top quark and antiquark production cross sections in the t channel and their ratio in proton-proton collisions at $\sqrt{s} = 13$ TeV", *Phys. Lett. B* **800** (2020) 135042, doi:10.1016/j.physletb.2019.135042, arXiv:1812.10514.

[55] CMS Collaboration, "Performance of electron reconstruction and selection with the CMS detector in proton-proton collisions at $\sqrt{s} = 8\,\text{TeV}$", *JINST* **10** (2015) P06005, doi:10.1088/1748-0221/10/06/P06005, arXiv:1502.02701.

[56] CMS Collaboration, "Performance of the CMS muon detector and muon reconstruction with proton-proton collisions at $\sqrt{s} = 13$ TeV", *JINST* **13** (2018) P06015, doi:10.1088/1748-0221/13/06/P06015, arXiv:1804.04528.

[57] CMS Collaboration, "Performance of reconstruction and identification of τ leptons decaying to hadrons and ν_τ in pp collisions at $\sqrt{s} = 13$ TeV", *JINST* **13** (2018) P10005, doi:10.1088/1748-0221/13/10/P10005, arXiv:1809.02816.

[58] CMS Collaboration, "Identification of hadronic tau lepton decays using a deep neural network", *JINST* **17** (2022) P07023, doi:10.1088/1748-0221/17/07/P07023, arXiv:2201.08458.

[59] CMS Collaboration, "Measurement of Higgs boson production and properties in the WW Decay channel with leptonic final states", *JHEP* **01** (2014) 096, doi:10.1007/JHEP01(2014)096, arXiv:1312.1129.

[60] D. P. Kingma and J. Ba, "Adam: A method for stochastic optimization", *Proceedings of the 3rd International Conference for Learning Representations, San Diego, 2015* (2017) doi:10.48550/arXiv.1412.6980, arXiv:1412.6980.

[61] I. Goodfellow, Y. Bengio, and A. Courville, "Deep learning". MIT Press, 2016. http://www.deeplearningbook.org.

[62] A. J. Barr et al., "Guide to transverse projections and mass-constraining variables", *Phys. Rev. D* **84** (2011) 095031, doi:10.1103/PhysRevD.84.095031, arXiv:1105.2977.

[63] D. L. Rainwater, R. Szalapski, and D. Zeppenfeld, "Probing color singlet exchange in Z + two jet events at the CERN LHC", *Phys. Rev. D* **54** (1996) 6680, doi:10.1103/PhysRevD.54.6680, arXiv:hep-ph/9605444.

[64] G. Cowan, K. Cranmer, E. Gross, and O. Vitells, "Asymptotic formulae for likelihood-based tests of new physics", *Eur. Phys. J. C* **71** (2011) 1554, doi:10.1140/epjc/s10052-011-1554-0, arXiv:1007.1727. [Erratum: doi:10.1140/epjc/s10052-013-2501-z].

[65] CMS Collaboration, "The CMS statistical analysis and combination tool: COMBINE", 2024. arXiv:2404.06614. Submitted to *Comput. Softw. Big Sci.*

[66] W. Verkerke and D. Kirkby, "The roofit toolkit for data modeling", 2003. https://arxiv.org/abs/physics/0306116.

[67] L. Moneta et al., "The RooStats project", *PoS* **ACAT2010** (2010) 057, doi:10.22323/1.093.0057, arXiv:1009.1003.

[68] CMS Collaboration, "Precision luminosity measurement in proton-proton collisions at $\sqrt{s} = 13$ TeV in 2015 and 2016 at CMS", *Eur. Phys. J. C* **81** (2021) 800, doi:10.1140/epjc/s10052-021-09538-2, arXiv:2104.01927.

[69] CMS Collaboration, "CMS luminosity measurement for the 2017 data-taking period at $\sqrt{s} = 13$ TeV", CMS Physics Analysis Summary CMS-PAS-LUM-17-004, 2018.

[70] CMS Collaboration, "CMS luminosity measurement for the 2018 data-taking period at $\sqrt{s} = 13$ TeV", CMS Physics Analysis Summary CMS-PAS-LUM-18-002, 2019.

[71] A. Kalogeropoulos and J. Alwall, "The SysCalc code: A tool to derive theoretical systematic uncertainties", 2018. arXiv:1801.08401.

[72] J. Butterworth et al., "PDF4LHC recommendations for LHC Run II", *J. Phys. G* **43** (2016) 023001, doi:10.1088/0954-3899/43/2/023001, arXiv:1510.03865.

[73] CMS Collaboration, "Measurement of the inelastic proton-proton cross section at $\sqrt{s} = 13$ TeV", *JHEP* **07** (2018) 161, doi:10.1007/JHEP07(2018)161, arXiv:1802.02613.

[74] CMS Collaboration, "Performance of the CMS electromagnetic calorimeter in pp collisions at $\sqrt{s} = 13$ TeV", *JINST* **19** (2024) P09004, doi:10.1088/1748-0221/19/09/P09004, arXiv:2403.15518.

[75] CMS Collaboration, "Jet energy scale and resolution in the CMS experiment in pp collisions at 8 TeV", *JINST* **12** (2017) P02014, doi:10.1088/1748-0221/12/02/P02014, arXiv:1607.03663.

[76] J. S. Conway, "Incorporating nuisance parameters in likelihoods for multisource spectra", in *PHYSTAT 2011*, p. 115. 2011. arXiv:1103.0354. doi:10.5170/CERN-2011-006.115.

[77] HEPData record for this analysis, 2024. doi:10.17182/hepdata.154440.

A The CMS Collaboration

Yerevan Physics Institute, Yerevan, Armenia
A. Hayrapetyan, A. Tumasyan[1]

Institut für Hochenergiephysik, Vienna, Austria
W. Adam, J.W. Andrejkovic, T. Bergauer, S. Chatterjee, K. Damanakis, M. Dragicevic, P.S. Hussain, M. Jeitler[2], N. Krammer, A. Li, D. Liko, I. Mikulec, J. Schieck[2], R. Schöfbeck, D. Schwarz, M. Sonawane, W. Waltenberger, C.-E. Wulz[2]

Universiteit Antwerpen, Antwerpen, Belgium
T. Janssen, T. Van Laer, P. Van Mechelen

Vrije Universiteit Brussel, Brussel, Belgium
N. Breugelmans, J. D'Hondt, S. Dansana, A. De Moor, M. Delcourt, F. Heyen, S. Lowette, I. Makarenko, D. Müller, S. Tavernier, M. Tytgat[3], G.P. Van Onsem, S. Van Putte, D. Vannerom

Université Libre de Bruxelles, Bruxelles, Belgium
B. Bilin, B. Clerbaux, A.K. Das, G. De Lentdecker, H. Evard, L. Favart, P. Gianneios, J. Jaramillo, A. Khalilzadeh, F.A. Khan, K. Lee, M. Mahdavikhorrami, A. Malara, S. Paredes, M.A. Shahzad, L. Thomas, M. Vanden Bemden, C. Vander Velde, P. Vanlaer

Ghent University, Ghent, Belgium
M. De Coen, D. Dobur, G. Gokbulut, Y. Hong, J. Knolle, L. Lambrecht, D. Marckx, K. Mota Amarilo, A. Samalan, K. Skovpen, N. Van Den Bossche, J. van der Linden, L. Wezenbeek

Université Catholique de Louvain, Louvain-la-Neuve, Belgium
A. Benecke, A. Bethani, G. Bruno, C. Caputo, J. De Favereau De Jeneret, C. Delaere, I.S. Donertas, A. Giammanco, A.O. Guzel, Sa. Jain, V. Lemaitre, J. Lidrych, P. Mastrapasqua, T.T. Tran, S. Wertz

Centro Brasileiro de Pesquisas Fisicas, Rio de Janeiro, Brazil
G.A. Alves, M. Alves Gallo Pereira, E. Coelho, G. Correia Silva, C. Hensel, T. Menezes De Oliveira, C. Mora Herrera[4], A. Moraes, P. Rebello Teles, M. Soeiro, A. Vilela Pereira[4]

Universidade do Estado do Rio de Janeiro, Rio de Janeiro, Brazil
W.L. Aldá Júnior, M. Barroso Ferreira Filho, H. Brandao Malbouisson, W. Carvalho, J. Chinellato[5], E.M. Da Costa, G.G. Da Silveira[6], D. De Jesus Damiao, S. Fonseca De Souza, R. Gomes De Souza, M. Macedo, J. Martins[7], L. Mundim, H. Nogima, J.P. Pinheiro, A. Santoro, A. Sznajder, M. Thiel

Universidade Estadual Paulista, Universidade Federal do ABC, São Paulo, Brazil
C.A. Bernardes[6], L. Calligaris, T.R. Fernandez Perez Tomei, E.M. Gregores, I. Maietto Silverio, P.G. Mercadante, S.F. Novaes, B. Orzari, Sandra S. Padula

Institute for Nuclear Research and Nuclear Energy, Bulgarian Academy of Sciences, Sofia, Bulgaria
A. Aleksandrov, G. Antchev, R. Hadjiiska, P. Iaydjiev, M. Misheva, M. Shopova, G. Sultanov

University of Sofia, Sofia, Bulgaria
A. Dimitrov, L. Litov, B. Pavlov, P. Petkov, A. Petrov, E. Shumka

Instituto De Alta Investigación, Universidad de Tarapacá, Casilla 7 D, Arica, Chile
S. Keshri, D. Laroze, S. Thakur

Beihang University, Beijing, China
T. Cheng, T. Javaid, L. Yuan

Department of Physics, Tsinghua University, Beijing, China
Z. Hu, Z. Liang, J. Liu, K. Yi[8,9]

Institute of High Energy Physics, Beijing, China
G.M. Chen[10], H.S. Chen[10], M. Chen[10], F. Iemmi, C.H. Jiang, A. Kapoor[11], H. Liao, Z.-A. Liu[12], R. Sharma[13], J.N. Song[12], J. Tao, C. Wang[10], J. Wang, Z. Wang[10], H. Zhang, J. Zhao

State Key Laboratory of Nuclear Physics and Technology, Peking University, Beijing, China
A. Agapitos, Y. Ban, S. Deng, B. Guo, C. Jiang, A. Levin, C. Li, Q. Li, Y. Mao, S. Qian, S.J. Qian, X. Qin, X. Sun, D. Wang, H. Yang, L. Zhang, Y. Zhao, C. Zhou

Guangdong Provincial Key Laboratory of Nuclear Science and Guangdong-Hong Kong Joint Laboratory of Quantum Matter, South China Normal University, Guangzhou, China
S. Yang

Sun Yat-Sen University, Guangzhou, China
Z. You

University of Science and Technology of China, Hefei, China
K. Jaffel, N. Lu

Nanjing Normal University, Nanjing, China
G. Bauer[14], B. Li, J. Zhang

Institute of Modern Physics and Key Laboratory of Nuclear Physics and Ion-beam Application (MOE) - Fudan University, Shanghai, China
X. Gao[15], Y. Li

Zhejiang University, Hangzhou, Zhejiang, China
Z. Lin, C. Lu, M. Xiao

Universidad de Los Andes, Bogota, Colombia
C. Avila, D.A. Barbosa Trujillo, A. Cabrera, C. Florez, J. Fraga, J.A. Reyes Vega

Universidad de Antioquia, Medellin, Colombia
F. Ramirez, C. Rendón, M. Rodriguez, A.A. Ruales Barbosa, J.D. Ruiz Alvarez

University of Split, Faculty of Electrical Engineering, Mechanical Engineering and Naval Architecture, Split, Croatia
D. Giljanovic, N. Godinovic, D. Lelas, A. Sculac

University of Split, Faculty of Science, Split, Croatia
M. Kovac, A. Petkovic, T. Sculac

Institute Rudjer Boskovic, Zagreb, Croatia
P. Bargassa, V. Brigljevic, B.K. Chitroda, D. Ferencek, K. Jakovcic, S. Mishra, A. Starodumov[16], T. Susa

University of Cyprus, Nicosia, Cyprus
A. Attikis, K. Christoforou, A. Hadjiagapiou, C. Leonidou, J. Mousa, C. Nicolaou, L. Paizanos, F. Ptochos, P.A. Razis, H. Rykaczewski, H. Saka, A. Stepennov

Charles University, Prague, Czech Republic
M. Finger, M. Finger Jr., A. Kveton

Universidad San Francisco de Quito, Quito, Ecuador
E. Carrera Jarrin

Academy of Scientific Research and Technology of the Arab Republic of Egypt, Egyptian Network of High Energy Physics, Cairo, Egypt
A.A. Abdelalim[17,18], S. Elgammal[19], A. Ellithi Kamel[20]

Center for High Energy Physics (CHEP-FU), Fayoum University, El-Fayoum, Egypt
M. Abdullah Al-Mashad, M.A. Mahmoud

National Institute of Chemical Physics and Biophysics, Tallinn, Estonia
K. Ehataht, M. Kadastik, T. Lange, S. Nandan, C. Nielsen, J. Pata, M. Raidal, L. Tani, C. Veelken

Department of Physics, University of Helsinki, Helsinki, Finland
H. Kirschenmann, K. Osterberg, M. Voutilainen

Helsinki Institute of Physics, Helsinki, Finland
S. Bharthuar, N. Bin Norjoharuddeen, E. Brücken, F. Garcia, P. Inkaew, K.T.S. Kallonen, T. Lampén, K. Lassila-Perini, S. Lehti, T. Lindén, L. Martikainen, M. Myllymäki, M.m. Rantanen, H. Siikonen, J. Tuominiemi

Lappeenranta-Lahti University of Technology, Lappeenranta, Finland
P. Luukka, H. Petrow

IRFU, CEA, Université Paris-Saclay, Gif-sur-Yvette, France
M. Besancon, F. Couderc, M. Dejardin, D. Denegri, J.L. Faure, F. Ferri, S. Ganjour, P. Gras, G. Hamel de Monchenault, M. Kumar, V. Lohezic, J. Malcles, F. Orlandi, L. Portales, A. Rosowsky, M.Ö. Sahin, A. Savoy-Navarro[21], P. Simkina, M. Titov, M. Tornago

Laboratoire Leprince-Ringuet, CNRS/IN2P3, Ecole Polytechnique, Institut Polytechnique de Paris, Palaiseau, France
F. Beaudette, G. Boldrini, P. Busson, A. Cappati, C. Charlot, M. Chiusi, F. Damas, O. Davignon, A. De Wit, I.T. Ehle, B.A. Fontana Santos Alves, S. Ghosh, A. Gilbert, R. Granier de Cassagnac, A. Hakimi, B. Harikrishnan, L. Kalipoliti, G. Liu, M. Nguyen, C. Ochando, R. Salerno, J.B. Sauvan, Y. Sirois, L. Urda Gómez, E. Vernazza, A. Zabi, A. Zghiche

Université de Strasbourg, CNRS, IPHC UMR 7178, Strasbourg, France
J.-L. Agram[22], J. Andrea, D. Apparu, D. Bloch, J.-M. Brom, E.C. Chabert, C. Collard, S. Falke, U. Goerlach, R. Haeberle, A.-C. Le Bihan, M. Meena, O. Poncet, G. Saha, M.A. Sessini, P. Van Hove, P. Vaucelle

Centre de Calcul de l'Institut National de Physique Nucleaire et de Physique des Particules, CNRS/IN2P3, Villeurbanne, France
A. Di Florio

Institut de Physique des 2 Infinis de Lyon (IP2I), Villeurbanne, France

D. Amram, S. Beauceron, B. Blancon, G. Boudoul, N. Chanon, D. Contardo, P. Depasse, C. Dozen[23], H. El Mamouni, J. Fay, S. Gascon, M. Gouzevitch, C. Greenberg, G. Grenier, B. Ille, E. Jourd'huy, I.B. Laktineh, M. Lethuillier, L. Mirabito, S. Perries, A. Purohit, M. Vander Donckt, P. Verdier, J. Xiao

Georgian Technical University, Tbilisi, Georgia
I. Lomidze, T. Toriashvili[24], Z. Tsamalaidze[16]

RWTH Aachen University, I. Physikalisches Institut, Aachen, Germany
V. Botta, S. Consuegra Rodríguez, L. Feld, K. Klein, M. Lipinski, D. Meuser, A. Pauls, D. Pérez Adán, N. Röwert, M. Teroerde

RWTH Aachen University, III. Physikalisches Institut A, Aachen, Germany
S. Diekmann, A. Dodonova, N. Eich, D. Eliseev, F. Engelke, J. Erdmann, M. Erdmann, P. Fackeldey, B. Fischer, T. Hebbeker, K. Hoepfner, F. Ivone, A. Jung, M.y. Lee, F. Mausolf, M. Merschmeyer, A. Meyer, S. Mukherjee, D. Noll, F. Nowotny, A. Pozdnyakov, Y. Rath, W. Redjeb, F. Rehm, H. Reithler, V. Sarkisovi, A. Schmidt, C. Seth, A. Sharma, J.L. Spah, A. Stein, F. Torres Da Silva De Araujo[25], S. Wiedenbeck, S. Zaleski

RWTH Aachen University, III. Physikalisches Institut B, Aachen, Germany
C. Dziwok, G. Flügge, T. Kress, A. Nowack, O. Pooth, A. Stahl, T. Ziemons, A. Zotz

Deutsches Elektronen-Synchrotron, Hamburg, Germany
H. Aarup Petersen, M. Aldaya Martin, J. Alimena, S. Amoroso, Y. An, J. Bach, S. Baxter, M. Bayatmakou, H. Becerril Gonzalez, O. Behnke, A. Belvedere, F. Blekman[26], K. Borras[27], A. Campbell, A. Cardini, C. Cheng, F. Colombina, G. Eckerlin, D. Eckstein, L.I. Estevez Banos, O. Filatov, E. Gallo[26], A. Geiser, V. Guglielmi, M. Guthoff, A. Hinzmann, L. Jeppe, B. Kaech, M. Kasemann, C. Kleinwort, R. Kogler, M. Komm, D. Krücker, W. Lange, D. Leyva Pernia, K. Lipka[28], W. Lohmann[29], F. Lorkowski, R. Mankel, I.-A. Melzer-Pellmann, M. Mendizabal Morentin, A.B. Meyer, G. Milella, K. Moral Figueroa, A. Mussgiller, L.P. Nair, J. Niedziela, A. Nürnberg, Y. Otarid, J. Park, E. Ranken, A. Raspereza, D. Rastorguev, J. Rübenach, L. Rygaard, A. Saggio, M. Scham[30,27], S. Schnake[27], P. Schütze, C. Schwanenberger[26], D. Selivanova, K. Sharko, M. Shchedrolosiev, D. Stafford, F. Vazzoler, A. Ventura Barroso, R. Walsh, D. Wang, Q. Wang, Y. Wen, K. Wichmann, L. Wiens[27], C. Wissing, Y. Yang, A. Zimermmane Castro Santos

University of Hamburg, Hamburg, Germany
A. Albrecht, S. Albrecht, M. Antonello, S. Bein, L. Benato, S. Bollweg, M. Bonanomi, P. Connor, K. El Morabit, Y. Fischer, E. Garutti, A. Grohsjean, J. Haller, H.R. Jabusch, G. Kasieczka, P. Keicher, R. Klanner, W. Korcari, T. Kramer, C.c. Kuo, V. Kutzner, F. Labe, J. Lange, A. Lobanov, C. Matthies, L. Moureaux, M. Mrowietz, A. Nigamova, Y. Nissan, A. Paasch, K.J. Pena Rodriguez, T. Quadfasel, B. Raciti, M. Rieger, D. Savoiu, J. Schindler, P. Schleper, M. Schröder, J. Schwandt, M. Sommerhalder, H. Stadie, G. Steinbrück, A. Tews, M. Wolf

Karlsruher Institut fuer Technologie, Karlsruhe, Germany
S. Brommer, M. Burkart, E. Butz, T. Chwalek, A. Dierlamm, A. Droll, U. Elicabuk, N. Faltermann, M. Giffels, A. Gottmann, F. Hartmann[31], R. Hofsaess,

M. Horzela, U. Husemann, J. Kieseler, M. Klute, R. Koppenhöfer, J.M. Lawhorn, M. Link, A. Lintuluoto, B. Maier, S. Maier, S. Mitra, M. Mormile, Th. Müller, M. Neukum, M. Oh, E. Pfeffer, M. Presilla, G. Quast, K. Rabbertz, B. Regnery, N. Shadskiy, I. Shvetsov, H.J. Simonis, L. Sowa, L. Stockmeier, K. Tauqeer, M. Toms, N. Trevisani, R.F. Von Cube, M. Wassmer, S. Wieland, F. Wittig, R. Wolf, X. Zuo

Institute of Nuclear and Particle Physics (INPP), NCSR Demokritos, Aghia Paraskevi, Greece
G. Anagnostou, G. Daskalakis, A. Kyriakis, A. Papadopoulos[31], A. Stakia

National and Kapodistrian University of Athens, Athens, Greece
P. Kontaxakis, G. Melachroinos, Z. Painesis, I. Papavergou, I. Paraskevas, N. Saoulidou, K. Theofilatos, E. Tziaferi, K. Vellidis, I. Zisopoulos

National Technical University of Athens, Athens, Greece
G. Bakas, T. Chatzistavrou, G. Karapostoli, K. Kousouris, I. Papakrivopoulos, E. Siamarkou, G. Tsipolitis, A. Zacharopoulou

University of Ioánnina, Ioánnina, Greece
K. Adamidis, I. Bestintzanos, I. Evangelou, C. Foudas, C. Kamtsikis, P. Katsoulis, P. Kokkas, P.G. Kosmoglou Kioseoglou, N. Manthos, I. Papadopoulos, J. Strologas

HUN-REN Wigner Research Centre for Physics, Budapest, Hungary
C. Hajdu, D. Horvath[32,33], K. Márton, A.J. Rádl[34], F. Sikler, V. Veszpremi

MTA-ELTE Lendület CMS Particle and Nuclear Physics Group, Eötvös Loránd University, Budapest, Hungary
M. Csanád, K. Farkas, A. Fehérkuti[35], M.M.A. Gadallah[36], Á. Kadlecsik, P. Major, G. Pásztor, G.I. Veres

Faculty of Informatics, University of Debrecen, Debrecen, Hungary
B. Ujvari, G. Zilizi

HUN-REN ATOMKI - Institute of Nuclear Research, Debrecen, Hungary
G. Bencze, S. Czellar, J. Molnar, Z. Szillasi

Karoly Robert Campus, MATE Institute of Technology, Gyongyos, Hungary
T. Csorgo[35], F. Nemes[35], T. Novak

Panjab University, Chandigarh, India
S. Bansal, S.B. Beri, V. Bhatnagar, G. Chaudhary, S. Chauhan, N. Dhingra[37], A. Kaur, A. Kaur, H. Kaur, M. Kaur, S. Kumar, K. Sandeep, T. Sheokand, J.B. Singh, A. Singla

University of Delhi, Delhi, India
A. Ahmed, A. Bhardwaj, A. Chhetri, B.C. Choudhary, A. Kumar, A. Kumar, M. Naimuddin, K. Ranjan, M.K. Saini, S. Saumya

Saha Institute of Nuclear Physics, HBNI, Kolkata, India
S. Baradia, S. Barman[38], S. Bhattacharya, S. Das Gupta, S. Dutta, S. Dutta, S. Sarkar

Indian Institute of Technology Madras, Madras, India
M.M. Ameen, P.K. Behera, S.C. Behera, S. Chatterjee, G. Dash, P. Jana, P. Kalbhor, S. Kamble, J.R. Komaragiri[39], D. Kumar[39], P.R. Pujahari, N.R. Saha, A. Sharma, A.K. Sikdar, R.K. Singh, P. Verma, S. Verma, A. Vijay

Tata Institute of Fundamental Research-A, Mumbai, India
S. Dugad, G.B. Mohanty, B. Parida, M. Shelake, P. Suryadevara

Tata Institute of Fundamental Research-B, Mumbai, India
A. Bala, S. Banerjee, R.M. Chatterjee, M. Guchait, Sh. Jain, A. Jaiswal, S. Kumar, G. Majumder, K. Mazumdar, S. Parolia, A. Thachayath

National Institute of Science Education and Research, An OCC of Homi Bhabha National Institute, Bhubaneswar, Odisha, India
S. Bahinipati[40], C. Kar, D. Maity[41], P. Mal, T. Mishra, V.K. Muraleedharan Nair Bindhu[41], K. Naskar[41], A. Nayak[41], S. Nayak, K. Pal, P. Sadangi, S.K. Swain, S. Varghese[41], D. Vats[41]

Indian Institute of Science Education and Research (IISER), Pune, India
S. Acharya[42], A. Alpana, S. Dube, B. Gomber[42], P. Hazarika, B. Kansal, A. Laha, B. Sahu[42], S. Sharma, K.Y. Vaish

Isfahan University of Technology, Isfahan, Iran
H. Bakhshiansohi[43], A. Jafari[44], M. Zeinali[45]

Institute for Research in Fundamental Sciences (IPM), Tehran, Iran
S. Bashiri, S. Chenarani[46], S.M. Etesami, Y. Hosseini, M. Khakzad, E. Khazaie[47], M. Mohammadi Najafabadi, S. Tizchang[48]

University College Dublin, Dublin, Ireland
M. Felcini, M. Grunewald

INFN Sezione di Bari[a], Università di Bari[b], Politecnico di Bari[c], Bari, Italy
M. Abbrescia[a,b], A. Colaleo[a,b], D. Creanza[a,c], B. D'Anzi[a,b], N. De Filippis[a,c], M. De Palma[a,b], W. Elmetenawee[a,b,17], L. Fiore[a], G. Iaselli[a,c], L. Longo[a], M. Louka[a,b], G. Maggi[a,c], M. Maggi[a], I. Margjeka[a], V. Mastrapasqua[a,b], S. My[a,b], S. Nuzzo[a,b], A. Pellecchia[a,b], A. Pompili[a,b], G. Pugliese[a,c], R. Radogna[a,b], D. Ramos[a], A. Ranieri[a], L. Silvestris[a], F.M. Simone[a,c], Ü. Sözbilir[a], A. Stamerra[a,b], D. Troiano[a,b], R. Venditti[a,b], P. Verwilligen[a], A. Zaza[a,b]

INFN Sezione di Bologna[a], Università di Bologna[b], Bologna, Italy
G. Abbiendi[a], C. Battilana[a,b], D. Bonacorsi[a,b], P. Capiluppi[a,b], A. Castro[†a,b], F.R. Cavallo[a], M. Cuffiani[a,b], G.M. Dallavalle[a], T. Diotalevi[a,b], F. Fabbri[a], A. Fanfani[a,b], D. Fasanella[a], P. Giacomelli[a], L. Giommi[a,b], C. Grandi[a], L. Guiducci[a,b], S. Lo Meo[a,49], M. Lorusso[a,b], L. Lunerti[a], S. Marcellini[a], G. Masetti[a], F.L. Navarria[a,b], G. Paggi[a,b], A. Perrotta[a], F. Primavera[a,b], A.M. Rossi[a,b], S. Rossi Tisbeni[a,b], T. Rovelli[a,b], G.P. Siroli[a,b]

INFN Sezione di Catania[a], Università di Catania[b], Catania, Italy
S. Costa[a,b,50], A. Di Mattia[a], A. Lapertosa[a], R. Potenza[a,b], A. Tricomi[a,b,50], C. Tuve[a,b]

INFN Sezione di Firenze[a], Università di Firenze[b], Firenze, Italy
P. Assiouras[a], G. Barbagli[a], G. Bardelli[a,b], B. Camaiani[a,b], A. Cassese[a], R. Ceccarelli[a], V. Ciulli[a,b], C. Civinini[a], R. D'Alessandro[a,b], E. Focardi[a,b], T. Kello[a], G. Latino[a,b], P. Lenzi[a,b], M. Lizzo[a], M. Meschini[a], S. Paoletti[a], A. Papanastassiou[a,b], G. Sguazzoni[a], L. Viliani[a]

INFN Laboratori Nazionali di Frascati, Frascati, Italy
L. Benussi, S. Bianco, S. Meola[51], D. Piccolo

INFN Sezione di Genova[a]**, Università di Genova**[b]**, Genova, Italy**
P. Chatagnon[a], F. Ferro[a], E. Robutti[a], S. Tosi[a,b]

INFN Sezione di Milano-Bicocca[a]**, Università di Milano-Bicocca**[b]**, Milano, Italy**
A. Benaglia[a], F. Brivio[a], F. Cetorelli[a,b], F. De Guio[a,b], M.E. Dinardo[a,b], P. Dini[a], S. Gennai[a], R. Gerosa[a,b], A. Ghezzi[a,b], P. Govoni[a,b], L. Guzzi[a], M.T. Lucchini[a,b], M. Malberti[a], S. Malvezzi[a], A. Massironi[a], D. Menasce[a], L. Moroni[a], M. Paganoni[a,b], S. Palluotto[a,b], D. Pedrini[a], A. Perego[a,b], B.S. Pinolini[a], G. Pizzati[a,b], S. Ragazzi[a,b], T. Tabarelli de Fatis[a,b]

INFN Sezione di Napoli[a]**, Università di Napoli 'Federico II'**[b]**, Napoli, Italy; Università della Basilicata**[c]**, Potenza, Italy; Scuola Superiore Meridionale (SSM)**[d]**, Napoli, Italy**
S. Buontempo[a], A. Cagnotta[a,b], F. Carnevali[a,b], N. Cavallo[a,c], F. Fabozzi[a,c], A.O.M. Iorio[a,b], L. Lista[a,b,52], P. Paolucci[a,31], B. Rossi[a]

INFN Sezione di Padova[a]**, Università di Padova**[b]**, Padova, Italy; Università di Trento**[c]**, Trento, Italy**
R. Ardino[a], P. Azzi[a], N. Bacchetta[a,53], D. Bisello[a,b], P. Bortignon[a], G. Bortolato[a,b], A. Bragagnolo[a,b], A.C.M. Bulla[a], R. Carlin[a,b], T. Dorigo[a], F. Gasparini[a,b], U. Gasparini[a,b], S. Giorgetti[a], E. Lusiani[a], M. Margoni[a,b], A.T. Meneguzzo[a,b], M. Migliorini[a,b], M. Passaseo[a], J. Pazzini[a,b], P. Ronchese[a,b], R. Rossin[a,b], F. Simonetto[a,b], M. Tosi[a,b], A. Triossi[a,b], S. Ventura[a], M. Zanetti[a,b], P. Zotto[a,b], A. Zucchetta[a,b], G. Zumerle[a,b]

INFN Sezione di Pavia[a]**, Università di Pavia**[b]**, Pavia, Italy**
C. Aimè[a], A. Braghieri[a], S. Calzaferri[a], D. Fiorina[a], P. Montagna[a,b], V. Re[a], C. Riccardi[a,b], P. Salvini[a], I. Vai[a,b], P. Vitulo[a,b]

INFN Sezione di Perugia[a]**, Università di Perugia**[b]**, Perugia, Italy**
S. Ajmal[a,b], M.E. Ascioti[a,b], G.M. Bilei[a], C. Carrivale[a,b], D. Ciangottini[a,b], L. Fanò[a,b], M. Magherini[a,b], V. Mariani[a,b], M. Menichelli[a], F. Moscatelli[a,54], A. Rossi[a,b], A. Santocchia[a,b], D. Spiga[a], T. Tedeschi[a,b]

INFN Sezione di Pisa[a]**, Università di Pisa**[b]**, Scuola Normale Superiore di Pisa**[c]**, Pisa, Italy; Università di Siena**[d]**, Siena, Italy**
C.A. Alexe[a,c], P. Asenov[a,b], P. Azzurri[a], G. Bagliesi[a], R. Bhattacharya[a], L. Bianchini[a,b], T. Boccali[a], E. Bossini[a], D. Bruschini[a,c], R. Castaldi[a], M.A. Ciocci[a,b], M. Cipriani[a,b], V. D'Amante[a,d], R. Dell'Orso[a], S. Donato[a], A. Giassi[a], F. Ligabue[a,c], A.C. Marini[a], D. Matos Figueiredo[a], A. Messineo[a,b], M. Musich[a,b], F. Palla[a], A. Rizzi[a,b], G. Rolandi[a,c], S. Roy Chowdhury[a], T. Sarkar[a], A. Scribano[a], P. Spagnolo[a], R. Tenchini[a], G. Tonelli[a,b], N. Turini[a,d], F. Vaselli[a,c], A. Venturi[a], P.G. Verdini[a]

INFN Sezione di Roma[a]**, Sapienza Università di Roma**[b]**, Roma, Italy**
C. Baldenegro Barrera[a,b], P. Barria[a], C. Basile[a,b], F. Cavallari[a], L. Cunqueiro Mendez[a,b], D. Del Re[a,b], E. Di Marco[a,b], M. Diemoz[a], F. Errico[a,b], E. Longo[a,b], J. Mijuskovic[a,b], G. Organtini[a,b], F. Pandolfi[a], R. Paramatti[a,b], C. Quaranta[a,b], S. Rahatlou[a,b], C. Rovelli[a], F. Santanastasio[a,b], L. Soffi[a]

INFN Sezione di Torino[a]**, Università di Torino**[b]**, Torino, Italy; Università del Piemonte Orientale**[c]**, Novara, Italy**
N. Amapane[a,b], R. Arcidiacono[a,c], S. Argiro[a,b], M. Arneodo[a,c], N. Bartosik[a], R. Bellan[a,b], A. Bellora[a,b], C. Biino[a], C. Borca[a,b], N. Cartiglia[a], M. Costa[a,b],

R. Covarelli[a,b], N. Demaria[a], L. Finco[a], M. Grippo[a,b], B. Kiani[a,b], F. Legger[a], F. Luongo[a,b], C. Mariotti[a], L. Markovic[a,b], S. Maselli[a], A. Mecca[a,b], L. Menzio[a,b], P. Meridiani[a], E. Migliore[a,b], M. Monteno[a], R. Mulargia[a], M.M. Obertino[a,b], G. Ortona[a], L. Pacher[a,b], N. Pastrone[a], M. Pelliccioni[a], M. Ruspa[a,c], F. Siviero[a,b], V. Sola[a,b], A. Solano[a,b], A. Staiano[a], C. Tarricone[a,b], D. Trocino[a], G. Umoret[a,b], R. White[a,b]

INFN Sezione di Trieste[a], Università di Trieste[b], Trieste, Italy
J. Babbar[a,b], S. Belforte[a], V. Candelise[a,b], M. Casarsa[a], F. Cossutti[a], K. De Leo[a], G. Della Ricca[a,b]

Kyungpook National University, Daegu, Korea
S. Dogra, J. Hong, B. Kim, J. Kim, D. Lee, H. Lee, S.W. Lee, C.S. Moon, Y.D. Oh, M.S. Ryu, S. Sekmen, B. Tae, Y.C. Yang

Department of Mathematics and Physics - GWNU, Gangneung, Korea
M.S. Kim

Chonnam National University, Institute for Universe and Elementary Particles, Kwangju, Korea
G. Bak, P. Gwak, H. Kim, D.H. Moon

Hanyang University, Seoul, Korea
E. Asilar, J. Choi, D. Kim, T.J. Kim, J.A. Merlin, Y. Ryou

Korea University, Seoul, Korea
S. Choi, S. Han, B. Hong, K. Lee, K.S. Lee, S. Lee, J. Yoo

Kyung Hee University, Department of Physics, Seoul, Korea
J. Goh, S. Yang

Sejong University, Seoul, Korea
H. S. Kim, Y. Kim, S. Lee

Seoul National University, Seoul, Korea
J. Almond, J.H. Bhyun, J. Choi, J. Choi, W. Jun, J. Kim, S. Ko, H. Kwon, H. Lee, J. Lee, J. Lee, B.H. Oh, S.B. Oh, H. Seo, U.K. Yang, I. Yoon

University of Seoul, Seoul, Korea
W. Jang, D.Y. Kang, Y. Kang, S. Kim, B. Ko, J.S.H. Lee, Y. Lee, I.C. Park, Y. Roh, I.J. Watson

Yonsei University, Department of Physics, Seoul, Korea
S. Ha, H.D. Yoo

Sungkyunkwan University, Suwon, Korea
M. Choi, M.R. Kim, H. Lee, Y. Lee, I. Yu

College of Engineering and Technology, American University of the Middle East (AUM), Dasman, Kuwait
T. Beyrouthy, Y. Gharbia

Kuwait University - College of Science - Department of Physics, Safat, Kuwait
F. Alazemi

Riga Technical University, Riga, Latvia
K. Dreimanis, A. Gaile, C. Munoz Diaz, D. Osite, G. Pikurs, A. Potrebko, M. Seidel,

D. Sidiropoulos Kontos

University of Latvia (LU), Riga, Latvia
N.R. Strautnieks

Vilnius University, Vilnius, Lithuania
M. Ambrozas, A. Juodagalvis, A. Rinkevicius, G. Tamulaitis

National Centre for Particle Physics, Universiti Malaya, Kuala Lumpur, Malaysia
I. Yusuff[55], Z. Zolkapli

Universidad de Sonora (UNISON), Hermosillo, Mexico
J.F. Benitez, A. Castaneda Hernandez, H.A. Encinas Acosta, L.G. Gallegos Maríñez, M. León Coello, J.A. Murillo Quijada, A. Sehrawat, L. Valencia Palomo

Centro de Investigacion y de Estudios Avanzados del IPN, Mexico City, Mexico
G. Ayala, H. Castilla-Valdez, H. Crotte Ledesma, E. De La Cruz-Burelo, I. Heredia-De La Cruz[56], R. Lopez-Fernandez, J. Mejia Guisao, C.A. Mondragon Herrera, A. Sánchez Hernández

Universidad Iberoamericana, Mexico City, Mexico
C. Oropeza Barrera, D.L. Ramirez Guadarrama, M. Ramírez García

Benemerita Universidad Autonoma de Puebla, Puebla, Mexico
I. Bautista, I. Pedraza, H.A. Salazar Ibarguen, C. Uribe Estrada

University of Montenegro, Podgorica, Montenegro
I. Bubanja, N. Raicevic

University of Canterbury, Christchurch, New Zealand
P.H. Butler

National Centre for Physics, Quaid-I-Azam University, Islamabad, Pakistan
A. Ahmad, M.I. Asghar, A. Awais, M.I.M. Awan, H.R. Hoorani, W.A. Khan

AGH University of Krakow, Faculty of Computer Science, Electronics and Telecommunications, Krakow, Poland
V. Avati, L. Grzanka, M. Malawski

National Centre for Nuclear Research, Swierk, Poland
H. Bialkowska, M. Bluj, M. Górski, M. Kazana, M. Szleper, P. Zalewski

Institute of Experimental Physics, Faculty of Physics, University of Warsaw, Warsaw, Poland
K. Bunkowski, K. Doroba, A. Kalinowski, M. Konecki, J. Krolikowski, A. Muhammad

Warsaw University of Technology, Warsaw, Poland
K. Pozniak, W. Zabolotny

Laboratório de Instrumentação e Física Experimental de Partículas, Lisboa, Portugal
M. Araujo, D. Bastos, C. Beirão Da Cruz E Silva, A. Boletti, M. Bozzo, T. Camporesi, G. Da Molin, P. Faccioli, M. Gallinaro, J. Hollar, N. Leonardo, G.B. Marozzo, T. Niknejad, A. Petrilli, M. Pisano, J. Seixas, J. Varela, J.W. Wulff

Faculty of Physics, University of Belgrade, Belgrade, Serbia
P. Adzic, P. Milenovic

VINCA Institute of Nuclear Sciences, University of Belgrade, Belgrade, Serbia

D. Devetak, M. Dordevic, J. Milosevic, V. Rekovic

Centro de Investigaciones Energéticas Medioambientales y Tecnológicas (CIEMAT), Madrid, Spain
J. Alcaraz Maestre, Cristina F. Bedoya, J.A. Brochero Cifuentes, Oliver M. Carretero, M. Cepeda, M. Cerrada, N. Colino, B. De La Cruz, A. Delgado Peris, A. Escalante Del Valle, D. Fernández Del Val, J.P. Fernández Ramos, J. Flix, M.C. Fouz, O. Gonzalez Lopez, S. Goy Lopez, J.M. Hernandez, M.I. Josa, E. Martin Viscasillas, D. Moran, C. M. Morcillo Perez, Á. Navarro Tobar, C. Perez Dengra, A. Pérez-Calero Yzquierdo, J. Puerta Pelayo, I. Redondo, S. Sánchez Navas, J. Sastre, J. Vazquez Escobar

Universidad Autónoma de Madrid, Madrid, Spain
J.F. de Trocóniz

Universidad de Oviedo, Instituto Universitario de Ciencias y Tecnologías Espaciales de Asturias (ICTEA), Oviedo, Spain
B. Alvarez Gonzalez, J. Cuevas, J. Fernandez Menendez, S. Folgueras, I. Gonzalez Caballero, J.R. González Fernández, P. Leguina, E. Palencia Cortezon, J. Prado Pico, C. Ramón Álvarez, V. Rodríguez Bouza, A. Soto Rodríguez, A. Trapote, C. Vico Villalba, P. Vischia

Instituto de Física de Cantabria (IFCA), CSIC-Universidad de Cantabria, Santander, Spain
S. Bhowmik, S. Blanco Fernández, I.J. Cabrillo, A. Calderon, J. Duarte Campderros, M. Fernandez, G. Gomez, C. Lasaosa García, R. Lopez Ruiz, C. Martinez Rivero, P. Martinez Ruiz del Arbol, F. Matorras, P. Matorras Cuevas, E. Navarrete Ramos, J. Piedra Gomez, L. Scodellaro, I. Vila, J.M. Vizan Garcia

University of Colombo, Colombo, Sri Lanka
B. Kailasapathy[57], D.D.C. Wickramarathna

University of Ruhuna, Department of Physics, Matara, Sri Lanka
W.G.D. Dharmaratna[58], K. Liyanage, N. Perera

CERN, European Organization for Nuclear Research, Geneva, Switzerland
D. Abbaneo, C. Amendola, E. Auffray, G. Auzinger, J. Baechler, D. Barney, A. Bermúdez Martínez, M. Bianco, A.A. Bin Anuar, A. Bocci, L. Borgonovi, C. Botta, E. Brondolin, C. Caillol, G. Cerminara, N. Chernyavskaya, D. d'Enterria, A. Dabrowski, A. David, A. De Roeck, M.M. Defranchis, M. Deile, M. Dobson, G. Franzoni, W. Funk, S. Giani, D. Gigi, K. Gill, F. Glege, J. Hegeman, J.K. Heikkilä, B. Huber, V. Innocente, T. James, P. Janot, O. Kaluzinska, O. Karacheban[29], S. Laurila, P. Lecoq, E. Leutgeb, C. Lourenço, L. Malgeri, M. Mannelli, M. Matthewman, A. Mehta, F. Meijers, S. Mersi, E. Meschi, V. Milosevic, F. Monti, F. Moortgat, M. Mulders, I. Neutelings, S. Orfanelli, F. Pantaleo, G. Petrucciani, A. Pfeiffer, M. Pierini, H. Qu, D. Rabady, B. Ribeiro Lopes, M. Rovere, H. Sakulin, S. Sanchez Cruz, S. Scarfi, C. Schwick, M. Selvaggi, A. Sharma, K. Shchelina, P. Silva, P. Sphicas[59], A.G. Stahl Leiton, A. Steen, S. Summers, D. Treille, P. Tropea, D. Walter, J. Wanczyk[60], J. Wang, K.A. Wozniak[61], S. Wuchterl, P. Zehetner, P. Zejdl, W.D. Zeuner

Paul Scherrer Institut, Villigen, Switzerland
T. Bevilacqua[62], L. Caminada[62], A. Ebrahimi, W. Erdmann, R. Horisberger, Q. Ingram, H.C. Kaestli, D. Kotlinski, C. Lange, M. Missiroli[62], L. Noehte[62],

T. Rohe

ETH Zurich - Institute for Particle Physics and Astrophysics (IPA), Zurich, Switzerland
T.K. Aarrestad, K. Androsov[60], M. Backhaus, G. Bonomelli, A. Calandri, C. Cazzaniga, K. Datta, P. De Bryas Dexmiers D'archiac[60], A. De Cosa, G. Dissertori, M. Dittmar, M. Donegà, F. Eble, M. Galli, K. Gedia, F. Glessgen, C. Grab, N. Härringer, T.G. Harte, D. Hits, W. Lustermann, A.-M. Lyon, R.A. Manzoni, M. Marchegiani, L. Marchese, C. Martin Perez, A. Mascellani[60], F. Nessi-Tedaldi, F. Pauss, V. Perovic, S. Pigazzini, B. Ristic, F. Riti, R. Seidita, J. Steggemann[60], A. Tarabini, D. Valsecchi, R. Wallny

Universität Zürich, Zurich, Switzerland
C. Amsler[63], P. Bärtschi, M.F. Canelli, K. Cormier, M. Huwiler, W. Jin, A. Jofrehei, B. Kilminster, S. Leontsinis, S.P. Liechti, A. Macchiolo, P. Meiring, F. Meng, U. Molinatti, J. Motta, A. Reimers, P. Robmann, M. Senger, E. Shokr, F. Stäger, R. Tramontano

National Central University, Chung-Li, Taiwan
C. Adloff[64], D. Bhowmik, C.M. Kuo, W. Lin, P.K. Rout, P.C. Tiwari[39], S.S. Yu

National Taiwan University (NTU), Taipei, Taiwan
L. Ceard, K.F. Chen, P.s. Chen, Z.g. Chen, A. De Iorio, W.-S. Hou, T.h. Hsu, Y.w. Kao, S. Karmakar, G. Kole, Y.y. Li, R.-S. Lu, E. Paganis, X.f. Su, J. Thomas-Wilsker, L.s. Tsai, D. Tsionou, H.y. Wu, E. Yazgan

High Energy Physics Research Unit, Department of Physics, Faculty of Science, Chulalongkorn University, Bangkok, Thailand
C. Asawatangtrakuldee, N. Srimanobhas, V. Wachirapusitanand

Çukurova University, Physics Department, Science and Art Faculty, Adana, Turkey
D. Agyel, F. Boran, F. Dolek, I. Dumanoglu[65], E. Eskut, Y. Guler[66], E. Gurpinar Guler[66], C. Isik, O. Kara, A. Kayis Topaksu, U. Kiminsu, G. Onengut, K. Ozdemir[67], A. Polatoz, B. Tali[68], U.G. Tok, S. Turkcapar, E. Uslan, I.S. Zorbakir

Middle East Technical University, Physics Department, Ankara, Turkey
G. Sokmen, M. Yalvac[69]

Bogazici University, Istanbul, Turkey
B. Akgun, I.O. Atakisi, E. Gülmez, M. Kaya[70], O. Kaya[71], S. Tekten[72]

Istanbul Technical University, Istanbul, Turkey
A. Cakir, K. Cankocak[65,73], G.G. Dincer[65], Y. Komurcu, S. Sen[74]

Istanbul University, Istanbul, Turkey
O. Aydilek[75], B. Hacisahinoglu, I. Hos[76], B. Kaynak, S. Ozkorucuklu, O. Potok, H. Sert, C. Simsek, C. Zorbilmez

Yildiz Technical University, Istanbul, Turkey
S. Cerci[68], B. Isildak[77], D. Sunar Cerci, T. Yetkin

Institute for Scintillation Materials of National Academy of Science of Ukraine, Kharkiv, Ukraine
A. Boyaryntsev, B. Grynyov

National Science Centre, Kharkiv Institute of Physics and Technology, Kharkiv, Ukraine

L. Levchuk

University of Bristol, Bristol, United Kingdom
D. Anthony, J.J. Brooke, A. Bundock, F. Bury, E. Clement, D. Cussans, H. Flacher, M. Glowacki, J. Goldstein, H.F. Heath, M.-L. Holmberg, L. Kreczko, S. Paramesvaran, L. Robertshaw, S. Seif El Nasr-Storey, V.J. Smith, N. Stylianou[78], K. Walkingshaw Pass

Rutherford Appleton Laboratory, Didcot, United Kingdom
A.H. Ball, K.W. Bell, A. Belyaev[79], C. Brew, R.M. Brown, D.J.A. Cockerill, C. Cooke, A. Elliot, K.V. Ellis, K. Harder, S. Harper, J. Linacre, K. Manolopoulos, D.M. Newbold, E. Olaiya, D. Petyt, T. Reis, A.R. Sahasransu, G. Salvi, T. Schuh, C.H. Shepherd-Themistocleous, I.R. Tomalin, K.C. Whalen, T. Williams

Imperial College, London, United Kingdom
I. Andreou, R. Bainbridge, P. Bloch, C.E. Brown, O. Buchmuller, V. Cacchio, C.A. Carrillo Montoya, G.S. Chahal[80], D. Colling, J.S. Dancu, I. Das, P. Dauncey, G. Davies, J. Davies, M. Della Negra, S. Fayer, G. Fedi, G. Hall, M.H. Hassanshahi, A. Howard, G. Iles, C.R. Knight, J. Langford, J. León Holgado, L. Lyons, A.-M. Magnan, S. Mallios, M. Mieskolainen, J. Nash[81], M. Pesaresi, P.B. Pradeep, B.C. Radburn-Smith, A. Richards, A. Rose, K. Savva, C. Seez, R. Shukla, A. Tapper, K. Uchida, G.P. Uttley, L.H. Vage, T. Virdee[31], M. Vojinovic, N. Wardle, D. Winterbottom

Brunel University, Uxbridge, United Kingdom
K. Coldham, J.E. Cole, A. Khan, P. Kyberd, I.D. Reid

Baylor University, Waco, Texas, USA
S. Abdullin, A. Brinkerhoff, E. Collins, M.R. Darwish[82], J. Dittmann, K. Hatakeyama, J. Hiltbrand, B. McMaster, J. Samudio, S. Sawant, C. Sutantawibul, J. Wilson

Catholic University of America, Washington, DC, USA
R. Bartek, A. Dominguez, C. Huerta Escamilla, A.E. Simsek, R. Uniyal, A.M. Vargas Hernandez

The University of Alabama, Tuscaloosa, Alabama, USA
B. Bam, A. Buchot Perraguin, R. Chudasama, S.I. Cooper, C. Crovella, S.V. Gleyzer, E. Pearson, C.U. Perez, P. Rumerio[83], E. Usai, R. Yi

Boston University, Boston, Massachusetts, USA
A. Akpinar, C. Cosby, G. De Castro, Z. Demiragli, C. Erice, C. Fangmeier, C. Fernandez Madrazo, E. Fontanesi, D. Gastler, F. Golf, S. Jeon, J. O'cain, I. Reed, J. Rohlf, K. Salyer, D. Sperka, D. Spitzbart, I. Suarez, A. Tsatsos, A.G. Zecchinelli

Brown University, Providence, Rhode Island, USA
G. Benelli, D. Cutts, L. Gouskos, M. Hadley, U. Heintz, J.M. Hogan[84], T. Kwon, G. Landsberg, K.T. Lau, D. Li, J. Luo, S. Mondal, N. Pervan, T. Russell, S. Sagir[85], X. Shen, F. Simpson, M. Stamenkovic, N. Venkatasubramanian, X. Yan

University of California, Davis, Davis, California, USA
S. Abbott, C. Brainerd, R. Breedon, H. Cai, M. Calderon De La Barca Sanchez,

M. Chertok, M. Citron, J. Conway, P.T. Cox, R. Erbacher, F. Jensen, O. Kukral, G. Mocellin, M. Mulhearn, S. Ostrom, W. Wei, S. Yoo, F. Zhang

University of California, Los Angeles, California, USA
M. Bachtis, R. Cousins, A. Datta, G. Flores Avila, J. Hauser, M. Ignatenko, M.A. Iqbal, T. Lam, E. Manca, A. Nunez Del Prado, D. Saltzberg, V. Valuev

University of California, Riverside, Riverside, California, USA
R. Clare, J.W. Gary, M. Gordon, G. Hanson, W. Si

University of California, San Diego, La Jolla, California, USA
A. Aportela, A. Arora, J.G. Branson, S. Cittolin, S. Cooperstein, D. Diaz, J. Duarte, L. Giannini, Y. Gu, J. Guiang, R. Kansal, V. Krutelyov, R. Lee, J. Letts, M. Masciovecchio, F. Mokhtar, S. Mukherjee, M. Pieri, M. Quinnan, B.V. Sathia Narayanan, V. Sharma, M. Tadel, E. Vourliotis, F. Würthwein, Y. Xiang, A. Yagil

University of California, Santa Barbara - Department of Physics, Santa Barbara, California, USA
A. Barzdukas, L. Brennan, C. Campagnari, K. Downham, C. Grieco, J. Incandela, J. Kim, A.J. Li, P. Masterson, H. Mei, J. Richman, S.N. Santpur, U. Sarica, R. Schmitz, F. Setti, J. Sheplock, D. Stuart, T.Á. Vámi, S. Wang, D. Zhang

California Institute of Technology, Pasadena, California, USA
S. Bhattacharya, A. Bornheim, O. Cerri, A. Latorre, J. Mao, H.B. Newman, G. Reales Gutiérrez, M. Spiropulu, J.R. Vlimant, C. Wang, S. Xie, R.Y. Zhu

Carnegie Mellon University, Pittsburgh, Pennsylvania, USA
J. Alison, S. An, P. Bryant, M. Cremonesi, V. Dutta, T. Ferguson, T.A. Gómez Espinosa, A. Harilal, A. Kallil Tharayil, C. Liu, T. Mudholkar, S. Murthy, P. Palit, K. Park, M. Paulini, A. Roberts, A. Sanchez, W. Terrill

University of Colorado Boulder, Boulder, Colorado, USA
J.P. Cumalat, W.T. Ford, A. Hart, A. Hassani, G. Karathanasis, N. Manganelli, J. Pearkes, C. Savard, N. Schonbeck, K. Stenson, K.A. Ulmer, S.R. Wagner, N. Zipper, D. Zuolo

Cornell University, Ithaca, New York, USA
J. Alexander, S. Bright-Thonney, X. Chen, D.J. Cranshaw, J. Fan, X. Fan, S. Hogan, P. Kotamnives, J. Monroy, M. Oshiro, J.R. Patterson, M. Reid, A. Ryd, J. Thom, P. Wittich, R. Zou

Fermi National Accelerator Laboratory, Batavia, Illinois, USA
M. Albrow, M. Alyari, O. Amram, G. Apollinari, A. Apresyan, L.A.T. Bauerdick, D. Berry, J. Berryhill, P.C. Bhat, K. Burkett, J.N. Butler, A. Canepa, G.B. Cerati, H.W.K. Cheung, F. Chlebana, G. Cummings, J. Dickinson, I. Dutta, V.D. Elvira, Y. Feng, J. Freeman, A. Gandrakota, Z. Gecse, L. Gray, D. Green, A. Grummer, S. Grünendahl, D. Guerrero, O. Gutsche, R.M. Harris, R. Heller, T.C. Herwig, J. Hirschauer, B. Jayatilaka, S. Jindariani, M. Johnson, U. Joshi, T. Klijnsma, B. Klima, K.H.M. Kwok, S. Lammel, D. Lincoln, R. Lipton, T. Liu, C. Madrid, K. Maeshima, C. Mantilla, D. Mason, P. McBride, P. Merkel, S. Mrenna, S. Nahn, J. Ngadiuba, D. Noonan, S. Norberg, V. Papadimitriou, N. Pastika, K. Pedro, C. Pena[86], F. Ravera, A. Reinsvold Hall[87], L. Ristori, M. Safdari, E. Sexton-Kennedy, N. Smith, A. Soha, L. Spiegel, S. Stoynev, J. Strait,

L. Taylor, S. Tkaczyk, N.V. Tran, L. Uplegger, E.W. Vaandering, I. Zoi

University of Florida, Gainesville, Florida, USA
C. Aruta, P. Avery, D. Bourilkov, P. Chang, V. Cherepanov, R.D. Field, C. Huh, E. Koenig, M. Kolosova, J. Konigsberg, A. Korytov, K. Matchev, N. Menendez, G. Mitselmakher, K. Mohrman, A. Muthirakalayil Madhu, N. Rawal, S. Rosenzweig, Y. Takahashi, J. Wang

Florida State University, Tallahassee, Florida, USA
T. Adams, A. Al Kadhim, A. Askew, S. Bower, V. Hagopian, R. Hashmi, R.S. Kim, S. Kim, T. Kolberg, G. Martinez, H. Prosper, P.R. Prova, M. Wulansatiti, R. Yohay, J. Zhang

Florida Institute of Technology, Melbourne, Florida, USA
B. Alsufyani, M.M. Baarmand, S. Butalla, S. Das, T. Elkafrawy[88], M. Hohlmann, E. Yanes

University of Illinois Chicago, Chicago, Illinois, USA
M.R. Adams, A. Baty, C. Bennett, R. Cavanaugh, R. Escobar Franco, O. Evdokimov, C.E. Gerber, M. Hawksworth, A. Hingrajiya, D.J. Hofman, J.h. Lee, D. S. Lemos, A.H. Merrit, C. Mills, S. Nanda, G. Oh, B. Ozek, D. Pilipovic, R. Pradhan, E. Prifti, T. Roy, S. Rudrabhatla, M.B. Tonjes, N. Varelas, M.A. Wadud, Z. Ye, J. Yoo

The University of Iowa, Iowa City, Iowa, USA
M. Alhusseini, D. Blend, K. Dilsiz[89], L. Emediato, G. Karaman, O.K. Köseyan, J.-P. Merlo, A. Mestvirishvili[90], O. Neogi, H. Ogul[91], Y. Onel, A. Penzo, C. Snyder, E. Tiras[92]

Johns Hopkins University, Baltimore, Maryland, USA
B. Blumenfeld, L. Corcodilos, J. Davis, A.V. Gritsan, L. Kang, S. Kyriacou, P. Maksimovic, M. Roguljic, J. Roskes, S. Sekhar, M. Swartz

The University of Kansas, Lawrence, Kansas, USA
A. Abreu, L.F. Alcerro Alcerro, J. Anguiano, S. Arteaga Escatel, P. Baringer, A. Bean, Z. Flowers, D. Grove, J. King, G. Krintiras, M. Lazarovits, C. Le Mahieu, J. Marquez, M. Murray, M. Nickel, M. Pitt, S. Popescu[93], C. Rogan, C. Royon, R. Salvatico, S. Sanders, C. Smith, G. Wilson

Kansas State University, Manhattan, Kansas, USA
B. Allmond, R. Gujju Gurunadha, A. Ivanov, K. Kaadze, Y. Maravin, J. Natoli, D. Roy, G. Sorrentino

University of Maryland, College Park, Maryland, USA
A. Baden, A. Belloni, J. Bistany-riebman, Y.M. Chen, S.C. Eno, N.J. Hadley, S. Jabeen, R.G. Kellogg, T. Koeth, B. Kronheim, Y. Lai, S. Lascio, A.C. Mignerey, S. Nabili, C. Palmer, C. Papageorgakis, M.M. Paranjpe, E. Popova[94], A. Shevelev, L. Wang

Massachusetts Institute of Technology, Cambridge, Massachusetts, USA
J. Bendavid, I.A. Cali, P.c. Chou, M. D'Alfonso, J. Eysermans, C. Freer, G. Gomez-Ceballos, M. Goncharov, G. Grosso, P. Harris, D. Hoang, D. Kovalskyi, J. Krupa, L. Lavezzo, Y.-J. Lee, K. Long, C. Mcginn, A. Novak, M.I. Park, C. Paus, C. Reissel, C. Roland, G. Roland, S. Rothman, G.S.F. Stephans,

Z. Wang, B. Wyslouch, T. J. Yang

University of Minnesota, Minneapolis, Minnesota, USA
B. Crossman, B.M. Joshi, C. Kapsiak, M. Krohn, D. Mahon, J. Mans, B. Marzocchi, M. Revering, R. Rusack, R. Saradhy, N. Strobbe

University of Nebraska-Lincoln, Lincoln, Nebraska, USA
K. Bloom, D.R. Claes, G. Haza, J. Hossain, C. Joo, I. Kravchenko, J.E. Siado, W. Tabb, A. Vagnerini, A. Wightman, F. Yan, D. Yu

State University of New York at Buffalo, Buffalo, New York, USA
H. Bandyopadhyay, L. Hay, H.w. Hsia, I. Iashvili, A. Kalogeropoulos, A. Kharchilava, M. Morris, D. Nguyen, J. Pekkanen, S. Rappoccio, H. Rejeb Sfar, A. Williams, P. Young

Northeastern University, Boston, Massachusetts, USA
G. Alverson, E. Barberis, J. Bonilla, M. Campana, J. Dervan, Y. Haddad, Y. Han, A. Krishna, J. Li, M. Lu, G. Madigan, R. Mccarthy, D.M. Morse, V. Nguyen, T. Orimoto, A. Parker, L. Skinnari, D. Wood

Northwestern University, Evanston, Illinois, USA
J. Bueghly, S. Dittmer, K.A. Hahn, Y. Liu, Y. Miao, D.G. Monk, M.H. Schmitt, A. Taliercio, M. Velasco

University of Notre Dame, Notre Dame, Indiana, USA
G. Agarwal, R. Band, R. Bucci, S. Castells, A. Das, R. Goldouzian, M. Hildreth, K.W. Ho, K. Hurtado Anampa, T. Ivanov, C. Jessop, K. Lannon, J. Lawrence, N. Loukas, L. Lutton, J. Mariano, N. Marinelli, I. Mcalister, T. McCauley, C. Mcgrady, C. Moore, Y. Musienko[16], H. Nelson, M. Osherson, A. Piccinelli, R. Ruchti, A. Townsend, Y. Wan, M. Wayne, H. Yockey, M. Zarucki, L. Zygala

The Ohio State University, Columbus, Ohio, USA
A. Basnet, B. Bylsma, M. Carrigan, L.S. Durkin, C. Hill, M. Joyce, M. Nunez Ornelas, K. Wei, B.L. Winer, B. R. Yates

Princeton University, Princeton, New Jersey, USA
H. Bouchamaoui, P. Das, G. Dezoort, P. Elmer, A. Frankenthal, B. Greenberg, N. Haubrich, K. Kennedy, G. Kopp, S. Kwan, D. Lange, A. Loeliger, D. Marlow, I. Ojalvo, J. Olsen, D. Stickland, C. Tully

University of Puerto Rico, Mayaguez, Puerto Rico, USA
S. Malik

Purdue University, West Lafayette, Indiana, USA
A.S. Bakshi, S. Chandra, R. Chawla, A. Gu, L. Gutay, M. Jones, A.W. Jung, A.M. Koshy, M. Liu, G. Negro, N. Neumeister, G. Paspalaki, S. Piperov, V. Scheurer, J.F. Schulte, M. Stojanovic, J. Thieman, A. K. Virdi, F. Wang, A. Wildridge, W. Xie, Y. Yao

Purdue University Northwest, Hammond, Indiana, USA
J. Dolen, N. Parashar, A. Pathak

Rice University, Houston, Texas, USA
D. Acosta, T. Carnahan, K.M. Ecklund, P.J. Fernández Manteca, S. Freed, P. Gardner, F.J.M. Geurts, I. Krommydas, W. Li, J. Lin, O. Miguel Colin, B.P. Padley,

R. Redjimi, J. Rotter, E. Yigitbasi, Y. Zhang

University of Rochester, Rochester, New York, USA
A. Bodek, P. de Barbaro, R. Demina, J.L. Dulemba, A. Garcia-Bellido, O. Hindrichs, A. Khukhunaishvili, N. Parmar, P. Parygin[94], R. Taus

Rutgers, The State University of New Jersey, Piscataway, New Jersey, USA
B. Chiarito, J.P. Chou, S.V. Clark, D. Gadkari, Y. Gershtein, E. Halkiadakis, M. Heindl, C. Houghton, D. Jaroslawski, S. Konstantinou, I. Laflotte, A. Lath, R. Montalvo, K. Nash, J. Reichert, H. Routray, P. Saha, S. Salur, S. Schnetzer, S. Somalwar, R. Stone, S.A. Thayil, S. Thomas, J. Vora, H. Wang

University of Tennessee, Knoxville, Tennessee, USA
D. Ally, A.G. Delannoy, S. Fiorendi, S. Higginbotham, T. Holmes, A.R. Kanuganti, N. Karunarathna, L. Lee, E. Nibigira, S. Spanier

Texas A&M University, College Station, Texas, USA
D. Aebi, M. Ahmad, T. Akhter, O. Bouhali[95], R. Eusebi, J. Gilmore, T. Huang, T. Kamon[96], H. Kim, S. Luo, R. Mueller, D. Overton, D. Rathjens, A. Safonov

Texas Tech University, Lubbock, Texas, USA
N. Akchurin, J. Damgov, N. Gogate, V. Hegde, A. Hussain, Y. Kazhykarim, K. Lamichhane, S.W. Lee, A. Mankel, T. Peltola, I. Volobouev

Vanderbilt University, Nashville, Tennessee, USA
E. Appelt, Y. Chen, S. Greene, A. Gurrola, W. Johns, R. Kunnawalkam Elayavalli, A. Melo, F. Romeo, P. Sheldon, S. Tuo, J. Velkovska, J. Viinikainen

University of Virginia, Charlottesville, Virginia, USA
B. Cardwell, H. Chung, B. Cox, J. Hakala, R. Hirosky, A. Ledovskoy, C. Neu

Wayne State University, Detroit, Michigan, USA
S. Bhattacharya, P.E. Karchin

University of Wisconsin - Madison, Madison, Wisconsin, USA
A. Aravind, S. Banerjee, K. Black, T. Bose, S. Dasu, I. De Bruyn, P. Everaerts, C. Galloni, H. He, M. Herndon, A. Herve, C.K. Koraka, A. Lanaro, R. Loveless, J. Madhusudanan Sreekala, A. Mallampalli, A. Mohammadi, S. Mondal, G. Parida, L. Pétré, D. Pinna, A. Savin, V. Shang, V. Sharma, W.H. Smith, D. Teague, H.F. Tsoi, W. Vetens, A. Warden

Authors affiliated with an institute or an international laboratory covered by a cooperation agreement with CERN
S. Afanasiev, V. Alexakhin, D. Budkouski, I. Golutvin[†], I. Gorbunov, V. Karjavine, V. Korenkov, A. Lanev, A. Malakhov, V. Matveev[97], V. Palichik, V. Perelygin, M. Savina, V. Shalaev, S. Shmatov, S. Shulha, V. Smirnov, O. Teryaev, N. Voytishin, B.S. Yuldashev[98], A. Zarubin, I. Zhizhin, G. Gavrilov, V. Golovtcov, Y. Ivanov, V. Kim[97], P. Levchenko[99], V. Murzin, V. Oreshkin, D. Sosnov, V. Sulimov, L. Uvarov, A. Vorobyev[†], Yu. Andreev, A. Dermenev, S. Gninenko, N. Golubev, A. Karneyeu, D. Kirpichnikov, M. Kirsanov, N. Krasnikov, I. Tlisova, A. Toropin, T. Aushev, V. Gavrilov, N. Lychkovskaya, A. Nikitenko[100,101], V. Popov, A. Zhokin, M. Chadeeva[97], R. Chistov[97], S. Polikarpov[97], V. Andreev, M. Azarkin, M. Kirakosyan, A. Terkulov, E. Boos, V. Bunichev, M. Dubinin[86], L. Dudko, V. Klyukhin, O. Kodolova[101], O. Lukina,

S. Obraztsov, M. Perfilov, V. Savrin, A. Snigirev, G. Vorotnikov, V. Blinov[97], T. Dimova[97], A. Kozyrev[97], O. Radchenko[97], Y. Skovpen[97], V. Kachanov, D. Konstantinov, S. Slabospitskii, A. Uzunian, A. Babaev, V. Borshch, D. Druzhkin[102]

Authors affiliated with an institute formerly covered by a cooperation agreement with CERN
V. Chekhovsky, V. Makarenko

†: Deceased
[1]Also at Yerevan State University, Yerevan, Armenia
[2]Also at TU Wien, Vienna, Austria
[3]Also at Ghent University, Ghent, Belgium
[4]Also at Universidade do Estado do Rio de Janeiro, Rio de Janeiro, Brazil
[5]Also at Universidade Estadual de Campinas, Campinas, Brazil
[6]Also at Federal University of Rio Grande do Sul, Porto Alegre, Brazil
[7]Also at UFMS, Nova Andradina, Brazil
[8]Also at Nanjing Normal University, Nanjing, China
[9]Now at The University of Iowa, Iowa City, Iowa, USA
[10]Also at University of Chinese Academy of Sciences, Beijing, China
[11]Also at China Center of Advanced Science and Technology, Beijing, China
[12]Also at University of Chinese Academy of Sciences, Beijing, China
[13]Also at China Spallation Neutron Source, Guangdong, China
[14]Now at Henan Normal University, Xinxiang, China
[15]Also at Université Libre de Bruxelles, Bruxelles, Belgium
[16]Also at an institute or an international laboratory covered by a cooperation agreement with CERN
[17]Also at Helwan University, Cairo, Egypt
[18]Now at Zewail City of Science and Technology, Zewail, Egypt
[19]Now at British University in Egypt, Cairo, Egypt
[20]Now at Cairo University, Cairo, Egypt
[21]Also at Purdue University, West Lafayette, Indiana, USA
[22]Also at Université de Haute Alsace, Mulhouse, France
[23]Also at Istinye University, Istanbul, Turkey
[24]Also at Tbilisi State University, Tbilisi, Georgia
[25]Also at The University of the State of Amazonas, Manaus, Brazil
[26]Also at University of Hamburg, Hamburg, Germany
[27]Also at RWTH Aachen University, III. Physikalisches Institut A, Aachen, Germany
[28]Also at Bergische University Wuppertal (BUW), Wuppertal, Germany
[29]Also at Brandenburg University of Technology, Cottbus, Germany
[30]Also at Forschungszentrum Jülich, Juelich, Germany
[31]Also at CERN, European Organization for Nuclear Research, Geneva, Switzerland
[32]Also at HUN-REN ATOMKI - Institute of Nuclear Research, Debrecen, Hungary
[33]Now at Universitatea Babes-Bolyai - Facultatea de Fizica, Cluj-Napoca, Romania
[34]Also at MTA-ELTE Lendület CMS Particle and Nuclear Physics Group, Eötvös Loránd University, Budapest, Hungary
[35]Also at HUN-REN Wigner Research Centre for Physics, Budapest, Hungary
[36]Also at Physics Department, Faculty of Science, Assiut University, Assiut, Egypt
[37]Also at Punjab Agricultural University, Ludhiana, India
[38]Also at University of Visva-Bharati, Santiniketan, India
[39]Also at Indian Institute of Science (IISc), Bangalore, India
[40]Also at IIT Bhubaneswar, Bhubaneswar, India

[41]Also at Institute of Physics, Bhubaneswar, India
[42]Also at University of Hyderabad, Hyderabad, India
[43]Also at Deutsches Elektronen-Synchrotron, Hamburg, Germany
[44]Also at Isfahan University of Technology, Isfahan, Iran
[45]Also at Sharif University of Technology, Tehran, Iran
[46]Also at Department of Physics, University of Science and Technology of Mazandaran, Behshahr, Iran
[47]Also at Department of Physics, Isfahan University of Technology, Isfahan, Iran
[48]Also at Department of Physics, Faculty of Science, Arak University, ARAK, Iran
[49]Also at Italian National Agency for New Technologies, Energy and Sustainable Economic Development, Bologna, Italy
[50]Also at Centro Siciliano di Fisica Nucleare e di Struttura Della Materia, Catania, Italy
[51]Also at Università degli Studi Guglielmo Marconi, Roma, Italy
[52]Also at Scuola Superiore Meridionale, Università di Napoli 'Federico II', Napoli, Italy
[53]Also at Fermi National Accelerator Laboratory, Batavia, Illinois, USA
[54]Also at Consiglio Nazionale delle Ricerche - Istituto Officina dei Materiali, Perugia, Italy
[55]Also at Department of Applied Physics, Faculty of Science and Technology, Universiti Kebangsaan Malaysia, Bangi, Malaysia
[56]Also at Consejo Nacional de Ciencia y Tecnología, Mexico City, Mexico
[57]Also at Trincomalee Campus, Eastern University, Sri Lanka, Nilaveli, Sri Lanka
[58]Also at Saegis Campus, Nugegoda, Sri Lanka
[59]Also at National and Kapodistrian University of Athens, Athens, Greece
[60]Also at Ecole Polytechnique Fédérale Lausanne, Lausanne, Switzerland
[61]Also at University of Vienna, Vienna, Austria
[62]Also at Universität Zürich, Zurich, Switzerland
[63]Also at Stefan Meyer Institute for Subatomic Physics, Vienna, Austria
[64]Also at Laboratoire d'Annecy-le-Vieux de Physique des Particules, IN2P3-CNRS, Annecy-le-Vieux, France
[65]Also at Near East University, Research Center of Experimental Health Science, Mersin, Turkey
[66]Also at Konya Technical University, Konya, Turkey
[67]Also at Izmir Bakircay University, Izmir, Turkey
[68]Also at Adiyaman University, Adiyaman, Turkey
[69]Also at Bozok Universitetesi Rektörlügü, Yozgat, Turkey
[70]Also at Marmara University, Istanbul, Turkey
[71]Also at Milli Savunma University, Istanbul, Turkey
[72]Also at Kafkas University, Kars, Turkey
[73]Now at Istanbul Okan University, Istanbul, Turkey
[74]Also at Hacettepe University, Ankara, Turkey
[75]Also at Erzincan Binali Yildirim University, Erzincan, Turkey
[76]Also at Istanbul University - Cerrahpasa, Faculty of Engineering, Istanbul, Turkey
[77]Also at Yildiz Technical University, Istanbul, Turkey
[78]Also at Vrije Universiteit Brussel, Brussel, Belgium
[79]Also at School of Physics and Astronomy, University of Southampton, Southampton, United Kingdom
[80]Also at IPPP Durham University, Durham, United Kingdom
[81]Also at Monash University, Faculty of Science, Clayton, Australia
[82]Also at Institute of Basic and Applied Sciences, Faculty of Engineering, Arab Academy for Science, Technology and Maritime Transport, Alexandria, Egypt

[83]Also at Università di Torino, Torino, Italy
[84]Also at Bethel University, St. Paul, Minnesota, USA
[85]Also at Karamanoğlu Mehmetbey University, Karaman, Turkey
[86]Also at California Institute of Technology, Pasadena, California, USA
[87]Also at United States Naval Academy, Annapolis, Maryland, USA
[88]Also at Ain Shams University, Cairo, Egypt
[89]Also at Bingol University, Bingol, Turkey
[90]Also at Georgian Technical University, Tbilisi, Georgia
[91]Also at Sinop University, Sinop, Turkey
[92]Also at Erciyes University, Kayseri, Turkey
[93]Also at Horia Hulubei National Institute of Physics and Nuclear Engineering (IFIN-HH), Bucharest, Romania
[94]Now at another institute or international laboratory covered by a cooperation agreement with CERN
[95]Also at Texas A&M University at Qatar, Doha, Qatar
[96]Also at Kyungpook National University, Daegu, Korea
[97]Also at another institute or international laboratory covered by a cooperation agreement with CERN
[98]Also at Institute of Nuclear Physics of the Uzbekistan Academy of Sciences, Tashkent, Uzbekistan
[99]Also at Northeastern University, Boston, Massachusetts, USA
[100]Also at Imperial College, London, United Kingdom
[101]Now at Yerevan Physics Institute, Yerevan, Armenia
[102]Also at Universiteit Antwerpen, Antwerpen, Belgium